

This is an Open Access document downloaded from ORCA, Cardiff University's institutional repository: <https://orca.cardiff.ac.uk/id/eprint/131299/>

This is the author's version of a work that was submitted to / accepted for publication.

Citation for final published version:

Gao, Yongsheng, Zhou, Dezhong, Lyu, Jing, A, Sigen, Xu, Qian, Newland, Ben , Matyjaszewski, Krzysztof, Tai, Hongyun and Wang, Wenxin 2020. Complex polymer architectures through free-radical polymerization of multivinyl monomers. *Nature Reviews Chemistry* 4 (4) , pp. 194-212. 10.1038/s41570-020-0170-7

Publishers page: <http://dx.doi.org/10.1038/s41570-020-0170-7>

Please note:

Changes made as a result of publishing processes such as copy-editing, formatting and page numbers may not be reflected in this version. For the definitive version of this publication, please refer to the published source. You are advised to consult the publisher's version if you wish to cite this paper.

This version is being made available in accordance with publisher policies. See <http://orca.cf.ac.uk/policies.html> for usage policies. Copyright and moral rights for publications made available in ORCA are retained by the copyright holders.



Physical sciences/Chemistry/Chemical synthesis/Polymer synthesis [URI /639/638/549/941]

Physical sciences/Chemistry/Polymer chemistry/Polymer characterization [URI /639/638/455/958]

### **Complex polymer architectures through free-radical polymerization of multivinyl monomers**

Yongsheng Gao,<sup>1,2†</sup> Dezhong Zhou,<sup>1,3†,\*</sup> Jing Lyu,<sup>1,4†</sup> Sigen A,<sup>1</sup> Qian Xu,<sup>1</sup> Ben Newland,<sup>5</sup> Krzysztof Matyjaszewski,<sup>6</sup> Hongyun Tai,<sup>7</sup> Wenxin Wang<sup>1,4 \*</sup>

<sup>1</sup> Charles Institute of Dermatology, School of Medicine, University College Dublin, Dublin 4, Ireland

<sup>2</sup> Present address: School of Engineering and Applied Sciences, Harvard University, Cambridge, MA 02138

<sup>3</sup> School of Chemical Engineering and Technology, Xi'an Jiaotong University, Xi'an, Shaanxi 710049, China

<sup>4</sup> School of Mechanical and Materials Engineering, University College Dublin, Dublin 4, Ireland

<sup>5</sup> School of Pharmacy and Pharmaceutical Sciences, Cardiff University, Cardiff, CF10 3NB, UK

<sup>6</sup> Center for Macromolecular Engineering, Department of Chemistry, Carnegie Mellon University, Pittsburgh, Pennsylvania 15213, United States

<sup>7</sup> School of Chemistry, Bangor University, Deiniol Road, Bangor, Gwynedd LL57 2UW, U.K.

[dezhong.zhou@mail.xjtu.edu.cn](mailto:dezhong.zhou@mail.xjtu.edu.cn); [wenxin.wang@ucd.ie](mailto:wenxin.wang@ucd.ie)

**The construction of complex polymer architectures with well-defined topology, composition and functionality has been extensively explored as the molecular basis for the development of modern polymer materials. The unique reaction kinetics of free-radical polymerization leads to concurrent formation of crosslinks between polymer chains and rings within an individual chain and thus (co)polymerization of multivinyl monomers (MVMs) provides a facile method to manipulate chain topology and functionality. Regulating the relative contribution of these intermolecular and intramolecular chain propagation reactions is the key to the construction of architecturally complex polymers. This can be achieved through the design of new monomers or by spatially/kinetically controlling crosslinking reactions. These mechanisms enable the synthesis of various polymer architectures including linear, cyclized, branched and star-shaped polymer chains as well as crosslinked networks. In this Review, we highlight some of the contemporary experimental strategies to prepare complex polymer architectures using radical polymerization of MVMs. We also examine the recent development of characterization techniques for sub-chain connections in such complex macromolecules. Finally we discuss how these crosslinking reactions have been engineered to generate advanced polymer materials for use in a variety of biomedical applications.**

#### **[H1] Introduction**

The polymerization of vinyl monomers is one of the most extensively used chemical reactions; accounting for approximately half of annual worldwide synthetic polymer production (~334 million tons<sup>1</sup>).<sup>2,3</sup> To date, however, vinyl polymers have mainly been used as commodity plastics, rubbers and fibres. Inadequate control over molecular structure has been one of the key obstacles to expansion of the application spectrum of these materials. In particular, with the emergence of nano-, bio- and information technologies, the demand for more complex, well-defined and functionally specific polymer materials is rapidly increasing. In this context, chemists have developed methods to

access architecturally complex polymers with exquisite control over the connection of macromolecular chains.<sup>3,4</sup> The recent development of reversible deactivation radical polymerization (RDRP) reactions including atom transfer radical polymerization (ATRP), reversible addition–fragmentation chain-transfer (RAFT) polymerization, nitroxide-mediated radical polymerization,<sup>5–7</sup> have significantly improved our ability to control the homogeneity of chain length, the manner of chain propagation, and the chain-end functionality. This has paved the way for the synthesis of numerous types of architecturally complex polymer materials leaving one open question “How far can we push polymer architecture?”.<sup>8</sup>

Within this rapidly expanding field, we find that multifunctional vinyl monomers can play a substantial role in manipulating chain topology through the involvement of multiple reactive groups during the polymerization process. Various polymer architectures, for example, (hyper)branched, star, single-chain cyclized and network have been successfully created from this type of multifaceted monomer and are endowed with novel properties and functionalities for diverse applications including nanomedicine,<sup>9</sup> tissue engineering,<sup>10</sup> and catalysis.<sup>11</sup>

The history of radical polymerization of multivinyl monomers (MVMs) (Figure 1) can be traced back to 1935, when Staudinger and Husemann studied the free radical copolymerization (FRP) of divinylbenzene with styrene and for the first time proposed that the resulted product is a three-dimensional network macromolecule.<sup>12</sup> This work initiated the use of MVMs in the preparation of polymeric networks. In the 1940s, based on the mean-field gelation theory developed by Flory,<sup>13</sup> Stockmayer developed the first theoretical framework for networks from multivinyl/vinyl copolymerization system and provided the method for gel point calculation (Box 1).<sup>14</sup> Aside from the cyclopolymerization of special divinyl monomers which are a special case, the uncontrolled polymerization process and resulting rapid gelation at low monomer conversion limited the experimental advancement in this area until the emergence of the RDRP in the 1990s. Improved control over the chain propagating reactions and increasing sophistication in the design of the MVMs, have ultimately led to the development of several remarkable strategies for the production of complex polymeric architectures.

As shown in Box 2, the unique feature of radical polymerization of MVMs is that, together with monomer addition, there are two co-existing and competing crosslinking reactions: intramolecular cyclization and intermolecular crosslinking. The key to controlling such a polymerization reaction lies in tuning the occurrence of those two crosslinking reactions by either promoting the intermolecular crosslinking with minimum involvement of intramolecular cyclization or vice versa. The former strategy generates polymers with multiple inter-chain linkages and the latter, produces polymers rich in intra-chain rings.

In this Review, we highlight how the distinct polymeric structures can be designed by manipulating intermolecular and intramolecular crosslinking reactions during the radical polymerization of MVMs. In particular, we focus on the innovative strategies to delay the macroscopic gelation and new characterization techniques for distinguishing the inter-chain and intra-chain connections. Finally, we highlight the emerging biomedical applications of these architecturally complex polymers. We anticipate that this review will stimulate the new strategies for polymerization control, inspire more intriguing architectures, and expand the applications of such polymers.

## [H1] Inter-chain combination

In the decades following Staudinger and Husemann's description of the polymer network concept,<sup>12</sup> it has widely been agreed that the primary role of MVMs in FRP is to form a linkage between two different kinetic chains (Box 2). Such inter-chain combination function has provided easy access to synthetic polymers with crosslinked architectures, which are the foundation of various technologies, ranging from traditional chromatographic separation to recent expansion microscopy.<sup>15</sup> Aside from such crosslinked networks with an infinite molecular weight (MW), branched and star-like polymers with a finite MW are two other featured architectures from inter-chain combination. The gel point (the monomer conversion at the critical transition moment from a branched polymer to a network) and the extent of the competing intra-chain cyclization are the two critical parameters that must be controlled in the design, synthesis and characterization of the resulting polymer architectures.

## [H2] Crosslinked networks

Aside from a few special examples,<sup>16</sup> networks formed by FRP of MVMs suffer from structural inhomogeneity, (e.g. dangling, looped or entangled chains and chain/crosslink density fluctuation), which in turn greatly impacts their mechanical properties and limits their applications.<sup>17</sup> Non-ideal crosslinking kinetics, such as inefficient inter-chain crosslinking and extensive intra-chain cyclization, have been ascribed as the primary origins of structural defects.<sup>18</sup> Thus, one of the most challenging synthetic tasks for the production of ideal homogeneous MVM-derived network materials is to maximize the inter-chain crosslinking efficiency and eliminate the intra-chain cyclization, by manipulating the reaction conditions (Figure 2).

Research in the area are stymied by the lack of techniques to precisely characterize and quantify such intra-chain connections—the products of intra-chain cyclization reaction<sup>17</sup> (as shown in 'Characterization of chain connections' . Nevertheless, indirect evaluation of the extent of intra-chain cyclization has generally been done by analyzing a) the structure information of precursor polymers, for example MW and/or intrinsic viscosity, initial pendent vinyl conversion, b) gel points, c) network structural homogeneity, and d) network bulk properties, for example swellability and elongation and shear modulus, as well as through computational simulation.<sup>19–24</sup> Based on these techniques, reaction conditions and monomer structures that favor inter-chain crosslinking over intra-chain reactions have been reported. In the very early paper, Staudinger and Husemann<sup>12</sup> found that soluble polymers with low specific viscosity can be produced by polymerization of divinylbenzene in dilute conditions. This dilution effect was later explained by the relatively high and long lasting concentration of local pendent vinyl groups,<sup>25</sup> which results in enhanced **intramolecular cyclization [G]**. Similarly, solvent quality affects the crosslinking pathways: inter-chain combination is promoted in good solvents because of the excluded volume effects,<sup>26</sup> while intra-chain cyclization is favoured in poor solvent as a result of collapsed chain conformations.<sup>27</sup> Interestingly, Matsumoto and coworkers used this solvent quality effect to control the intermolecular crosslinking reactions by using divinyl monomers (DVMs) with opposite polarities to the primary chain. Intermolecular crosslinking reactions are promoted under conditions where crosslinkers could be assembled, but suppressed if the primary chains are assembled.<sup>28</sup> Tuning the MVM structure

(for example, the length of inter-vinyl spacers or functionality of MVMs), and concentration can also regulate the probabilities for intra-chain cyclization and inter-chain crosslinking reactions. For instance, using MVMs with larger inter-vinyl distance<sup>29,30</sup> or higher functionality<sup>31–33</sup> — the number of vinyl groups per monomers — generally increases the extent of inter-molecular crosslinking, leading to a more homogeneous network. Meanwhile, increasing the initial amount of DVM fed into an FRP system will tend to increase the crosslinking density to a degree, but the crosslinking density will stop at a plateau value or decrease with further increase of DVM concentration. This could be attributed to enhanced structural inhomogeneities<sup>22,34</sup>

These experimental approaches have paved the way for the development of structurally homogenous networks from MVM polymerization. However, conditions that provide only intermolecular crosslinking and entirely avoid intra-cyclization, thus producing structurally well-defined polymer networks, had not been reported until the recent work by Kitagawa and coworkers,<sup>16</sup> (Box 2c). DVMs were first embedding into the walls of metal-organic frameworks thus separating the two vinyl moieties in two different channels, subsequent polymerization reaction in the channels consumes the DVMs only by inter-chain crosslinking without any possibility for intra-chain cyclization. This elegant work enabled the production, for the first time, an ideal crosslinked network from radical polymerization with a well-positioned crosslinker and well-defined crosslink density and other unprecedented structural features such as: a) the linear primary chains were permanently aligned in parallel by tethering adjacent chains; b) the linear primary chains were kept in register at a predefined distance; c) pseudo-crystallinity was achieved in the presence of atactic polymer chains, which is unlikely to occur spontaneously for such polymers; d) the crosslinking was completely integrated into the pseudo-crystalline state; and e) the newly formed polymeric materials inherited the molecular and morphological hierarchical order of the host MOFs. However, the synthetic complexity and limited scalability has hindered wide application of such systems and more general methods towards such well-defined network are of great industrial and academic interest.

## **[H2] Branched polymers**

In branched polymers, oligomer subchains are interconnected to produce a globular macromolecule with a finite MW.<sup>35</sup> During radical polymerization of MVMs, the intermediate products prior to gelation are inherently branched, making this reaction a facile and cost-effective synthetic route towards branched polymers. Regulation (especially delay) of the gel point is key to achieve branched polymers with a reasonable yield.

**[H3] The “Strathclyde Route”.** Recall from the Flory–Stockmayer theory (Box 1), that the critical condition for the onset of gelation is when the weight-average number of crosslinked units per primary chain approaches unity. It logically follows that if the average number of crosslinks per kinetic chain is controlled to being small enough (i.e. < 1), soluble branched polymers may be readily obtained even at the full conversion (Figure 2b). The first experimental approach achieving this is known as the “Strathclyde Route” and was originally proposed by Sherrington and coworkers.<sup>36</sup> External chain transfer agents (CTAs) (Figure 3 A~H) were added to the conventional FRP of monovinyl monomers and DVMs in order to regulate both the primary chain length and the average number of crosslinks per

primary chain (Figure 3). In a typical reaction setup, the molar feed ratio of monovinyl monomers to DVMs to CTAs was set at 100:10:10, and soluble branched polymers were obtained at near-complete (~99% ) conversion.<sup>37,38</sup> This technique holds great industrial promise as a facile, pragmatic and cost-effective way to produce branched vinyl polymers using conventional FRP, especially so given later success demonstrated in aqueous emulsion,<sup>38</sup> solvent-free suspension<sup>39</sup> and continuous-flow reactors.<sup>40</sup>

In addition to the traditional thiol based CTAs, catalytic chain transfer agents were later used in a similar manner.<sup>41</sup> Given the reversible chain transfer feature of catalytic CTAs, the addition of a ppm level of bis[(difluoroboryl)dimethylglyoximate]cobalt(II) (CoBF) (Figure 3 I) was sufficient to massively suppress the intermolecular crosslinking and gelation, producing soluble branched polymers with monomer conversion over 90%.<sup>42</sup> It then became critical to optimize the concentration of catalytic CTAs employed as chain transfer rate constants were found to vary significantly between different catalytic CTA/monomer combinations. Smeets later described an empirically determined rule-of-thumb was that to prevent macroscopic gelation, the chain transfer frequency (defined as  $k_{tr} \times [CTA]$  in  $s^{-1}$ ) should be 85 times the DVMs fraction (in mol % relative to monovinyl monomers),<sup>43</sup> which is an important empirical parameter for the synthesis of branched polymers from such “Strathclyde route” polymerization processes.

In a conceptually similar manner to the “Strathclyde Route”, the addition of oxygen<sup>44</sup> or the use of large amounts of initiator<sup>45</sup> have also been used to terminate the propagation chain in conventional FRP of monovinyl monomer/DVM systems leading to gel-free branched polymers.

In RDRP systems (unlike conventional FRP), the average number of crosslinks per primary chain can be readily controlled by tuning the molar feed ratio of DVM:initiator (in the case of ATRP and nitroxide-mediated radical polymerization) or DVM:RAFT agent (for RAFT polymerization). This paves the way for the successful implementation of the “Strathclyde Route” to RDRP. Two prerequisite conditions are 1) the chain propagation must remain well-controlled in such crosslinking RDRP systems, as verified by both simulated and experimental data,<sup>46-49</sup> and 2) the observed values of DVM:primary chain should correlate well with the feed ratio.<sup>50</sup> Soluble branched polymers were obtained at near complete monomer conversion, provided that the feed ratio of DVM:initiator was kept around or less than 1.<sup>51-54</sup> In some cases, higher (up to 5) DVMs per primary chain can be tolerated without causing the macroscopic gelation at near full vinyl conversion, an observation which can be easily attributed to increasing the intramolecular cyclization.<sup>51,55</sup> Nevertheless, these approaches represent the design of a RDRP of monovinyl monomers/DVMs system with a gel point at or beyond the point of complete monomer conversion (Figure 2b), such that less than one divinyl branching monomer is incorporated into each primary chain at the end of the reaction, and thus leading to the formation of branched polymers in facile one-pot reactions.

**[H3] Deactivation-enhanced RDRP homopolymerization of MVMs.** In contrast to the ‘Strathclyde route’, which manipulates the number of MVMs per primary chain, the deactivation enhanced ATRP strategy controls the **instantaneous kinetic chain length [G]** in order to suppress uncontrolled crosslinking and thus delay the onset of

gelation. More importantly, this approach offers the possibility to homopolymerize MVMs at moderate or high concentration to synthesize soluble products in good yields without the necessity of elaborate monomer design.<sup>56</sup> In the original work, Wang and co-workers found that the addition of a large amount of deactivator in ATRP homopolymerization of common commercially available MVMs such as divinylbenzene and ethylene glycol dimethylacrylate, resulted in the significant increase in critical gel point (up to 60% monomer conversion).<sup>57</sup> This represents a marked improvement on the conventional ATRP system and is 5-fold higher than the predicted values by Flory–Stockmayer theory. Almost complete conversion (up to 96%)<sup>58</sup> was later achieved by feeding the deactivator and a small amount of reducing agent (e.g., ascorbic acid) to generate a small amount of activator *in situ*.<sup>59</sup>

As described in Box 3, the key to this approach is to control the polymerization kinetics. Deactivation-enhanced (DE) strategy features a much slower monomer addition rate ( $R_{pM}$ ) compared with the deactivation rate ( $R_{deact}$ ), leading to a small instantaneous kinetic chain length. The intuitive correlation of kinetic chain length with growth boundary make it easier to understand the DE effect. The small growth boundary confines chain growth so that the few closest vinyls have a much higher chance to be added to the active center during each activation/deactivation cycle, and hence keeps the polymer chains growing in a limited space (Figure 2d). This avoids the rapid formation of long polymer chains and the subsequent combinations of high MW chains in the early stages of the polymerization. With a small growth boundary, controlling the chances of chain overlaps (by, for example, manipulating the chain dimension and chain volume concentration) can potentially regulate the occurrence of intermolecular crosslinking and intramolecular cyclization, and thereby control the polymer architecture. This can be achieved by controlling the initial molar feed ratio of DVMs to initiator ( $N_k$ ). A small  $N_k$  value (e.g. 2) is needed to achieve a hyperbranched topology,<sup>59</sup> as MVMs are predominately converted to short oligomers under this condition (Box 3). The subsequent intermolecular combination produces hyperbranched polymers with a high degree of branching [G] and vinyl functional groups.

**[H3] Selective polymerization of asymmetric MVMs.** Delay of the gel point can be obtained by chemoselective polymerization of asymmetric MVMs which possess with two or more vinyl groups with different reactivity. The highly reactive vinyls are polymerized first (*via* the monomer addition pathway) leaving the less reactive to be consumed in a delayed manner or as pendent functional groups. As a result, branched or even linear polymers (as opposed to crosslinked networks) are expected from such reactions, provided the reactivity ratio for each pair of vinyl moieties ( $r_1/r_2$ , calculated based on Alfrey–Price theory<sup>60</sup>) is significantly different (Figure 4).<sup>61</sup> Attempts to chemoselectively polymerize two commercially available asymmetrical DVMs: vinyl methacrylate (Figure 4 A) and allyl methacrylate (Figure 4 B) in which the reactivity ratios of the two vinyl moieties are ~1700 and 28, respectively, using FRP or RDRP, showed a poor selectivity.<sup>62–64</sup> Asymmetric MVMs with much higher reactivity ratio such as 4-(3'-Buten-1'-oxy)-2,3,5,6-tetrafluorostyrene (Figure 4 E)<sup>65</sup> and 4-(cyclohex-3'-enylmethoxy)-2,3,5,6-tetrafluorostyrene (Figure 4 G)<sup>66</sup> with reactivity ratio of 8800 and 100,000, respectively, were later designed by Wooley and coworkers, and good chemoselectivity was achieved in such radical polymerization reactions, yielding linear polymers bearing pendent vinyls.<sup>65,66</sup>

As an alternative to the pursuit of absolute selectivity in the polymerization reaction, the occasional and asynchronous participation of the pendent vinyls during chain propagation can be exploited to synthesize soluble branched polymers

at higher monomer conversion (Figure 4 right).<sup>67,68</sup> For instance, RAFT homopolymerization of 2-(5-norbornene)methyl methacrylate (Figure 4 D) bearing a methacrylate group and a norbornene group with reactivity ratio about 160, produced soluble hyperbranched polymers at monomer conversion of 90% with < 3% residual methacrylate and ~67 - 83% residual norbornene, suggesting a branch ratio of ~17 - 33% was achieved.<sup>69</sup>

## **[H2] Star polymers**

Star polymers are another type of architecturally complex polymer, featuring multiple linear/dendritic arm chains radiating from a central core. These polymers have received significant attention in recent decades because their structures lead to nanosized objects with controllable topology and desirable functionalities. The structural features and synthetic strategies for the production of star polymers are very broad, and so readers are guided to a recent review.<sup>70</sup> Here, rather than summarizing again the approaches to star polymer formation, we focus on the controlling the addition timing of MVMs which is an exemplary strategy for controlling MVM polymerization that yields soluble products in high yield without macrogelation. The primary role of MVMs in the synthesis of star polymers is to connect multiple linear chain ends together, and can be achieved either by adding MVMs to crosslink preformed linear/dendritic chains (arm-first), or polymerizing MVMs first to a generate a crosslinked core, followed by the growth of linear chains (core-first), as shown in Figure 2c. This synthetic strategy can be generalized to the control of MVM addition timing, which governs the spatial distribution of crosslinking units. From this point of view, conventional monovinyl monomer/MVMs copolymerization for synthesizing insoluble macroscopic gels is a one-pot reaction with simultaneous addition of monovinyl monomers and MVMs.<sup>71</sup> The recent success in synthesizing soluble, branched polymers via semi-batch addition of MVM during RDRP (MVMs are added slowly during the reaction) of monovinyl monomers<sup>72,73</sup> further highlight this effect of MVM addition timing.

**[H3] The arm-first route.** In the arm-first route, pre-synthesized linear polymers (arms) bearing an  $\alpha$ - or  $\omega$ -chain-end reactive moiety (e.g. an initiator fragment<sup>74</sup> or vinyl group<sup>75</sup>) or dendritic polymers with a single functionality at the focal point<sup>76-78</sup> are subjected to localized crosslinking with the added MVMs. When the maximum number of arms is reached, the buildup of steric hindrance around the core, acts to hamper the star-star coupling and macrogelation, leading to soluble star-shaped final products.<sup>79</sup> The successful implementation of “arm-first” polymerization replies on the optimization of a large number of variables, including i) amount of DVM added; ii) the manner of DVM addition; iii) the chemical nature of DVM; iv) the degree of polymerization and chemical nature of the linear arms; v) the nature of the solvent and monomer concentration.<sup>80-83</sup> A large ratio MVMs per linear macroinitiators (5 ~ 20 in ATRP<sup>74,84</sup> or even higher in other reactions<sup>85</sup>) can be tolerated in such system. Recall, then, that from the Flory–Stockmayer theory, in the one-pot addition methods, the molar feed ratio of MVMs per primary chain needs to be less than unity to avoid macrogelation, highlighting the benefits of localized crosslinks in avoiding macrogelation.

**[H3] The core-first route.** DVMs were polymerized under ultra-dilute conditions to produce near monodisperse nano-objects with multiple reactivatable sites to facilitate the further linear chain growth. For instance, Gao and Matyjaszewski homopolymerized ethylene glycol diacrylate under dilute conditions to provide a soluble and



nanosized crosslinked gel containing multiple initiating moieties.<sup>86</sup> After most of the DVMs and pendent vinyl groups were consumed, a large amount of monovinyl monomers was added to perform the “grafting-from” polymerization [G] and produce star-like polymers. The key to this method is to keep the proportion of pendent vinyl groups per core at an extremely low level in order to prevent star–star coupling and eliminate the formation of “arm–star” loops. An advantage of such a “core-first” approach over the “arm-first” method is that the dormant initiating moieties are located at the star periphery, facilitating the further chain extension or chain end transformation.

### [H1] Intra-chain cyclization

To achieve an efficient intra-chain cyclization in multivinyl polymerization, the monomer design or conditions must be manipulated in order that it is kinetically favoured, i.e. cyclization rate is faster than the intermolecular reaction rate. This can be achieved by either shortening the intervinylic distance within a MVM (i.e. proximity effects) or shortening the growth boundary to ensure that the majority of pendent vinyls are located inside the growth boundary of the chain-end radicals from the same primary chain. Other general approaches favouring intra-chain cyclization such as decreasing monomer concentration, lowering solvent quality can also be combined with those strategies.

### [H2] Cyclopolymers

Cyclopolymers are soluble linear polymers with repeated in-chain cyclic units, obtained from multivinyl polymerization with alternating monomer addition and intra-chain cyclization in the absence of intermolecular crosslinking (Figure 5). The first example of cyclopolymerization was described by Butler and coworkers,<sup>87,88</sup> who found several unexpected water soluble products were produced in the FRP of diallyldimethylammonium salts. The historical development, the scope, the mechanism and the practical significance of cyclopolymerization have been summarized recently.<sup>89</sup> Here, we focus on the recently described monomer design strategies that facilitate intra-chain cyclization during radical cyclopolymerization.

**[H3] Five- and six-membered cycles.** The general principle of the monomer design for cyclopolymerization is to have the two vinyl groups spatially close for efficient intramolecular cyclization. As per the “5 Å rule [G]”,<sup>90</sup> smaller DVMs with a short intervinylic distance, such as unconjugated 1,5- and 1,6 dienes, are inherently desirable. Following Butler’s initial study on FRP of diallyldimethylammonium salts,<sup>87,88</sup> various 1,5- and 1,6 dienes such as (meth)acrylic anhydride,<sup>91</sup> divinyl acetals,<sup>92</sup> *o*-divinylbenzene<sup>93</sup> and diallylsilanes<sup>94</sup> were subjected to FRP and the structures obtained were demonstrated to have five- and six-membered rings (Figure 5a) distributed along the C–C chains. The rapid expansion of RDRP techniques in the last two decades have greatly facilitated the synthesis of cyclopolymers with well-defined MW, low dispersity and high chain end functionalities. For instance, Acar and coworkers reported the cyclopolymerization of *tert*-butyl  $\alpha$ -(hydroxymethyl) acrylate by both ATRP<sup>95</sup> and RAFT polymerization.<sup>96</sup> In both systems, the soluble polymers with six-membered tetrahydropyran repeat units were synthesized at high conversion (>80%) with low *D* and well-defined MW.

**[H3] Macrocycles.** The likelihood of intramolecular cyclization reactions occurring decreases significantly for rings larger than six atoms,<sup>97</sup> and extra effort must be expended to constrain the two or more polymerizable vinyl moieties in close proximity for cyclopolymerization.

The use of chiral or bulky moieties as template molecules that regulate the vinyl orientation and enhance cyclization, was one of the earliest strategies applied to produce cyclopolymers with macrocycles.<sup>98–102</sup> For example, the conformationally locked structure of *myo*-inositol orthoformate, which orients two hydroxyl groups in axial positions of a six-membered ring, was used as the template molecule to generate a 4,6-bis(4-vinyl)-benzyl-*myo*-inositol orthoformate (Figure 5, **7**) resulting in an intervinylic distance of about 4–5 Å.<sup>103,104</sup> Radical cyclopolymerization of these monomers under high dilution (0.1 M) produced soluble products with a high yield (80–90%). In a recent study, the Thorpe–Ingold or gem-dimethyl effect has been applied by Li and co-workers to promote the cyclization of dimethacrylate and bisstyrenic groups (Figure 5, **10** and **14**) with RAFT cyclopolymerization producing a quasi-double-helical cyclopolymer with switchable chirality.<sup>105</sup>

Hydrogen bonding can also be exploited to tether and orient vinyl groups, either by using a template molecule such as a catechol (Figure 5, **17**)<sup>106</sup> to tether two vinyl monomers, or connecting two vinyl monomers with complementary hydrogen bonding moieties (Figure 5, **16**).<sup>107</sup> While these pseudo-DVMs can assist in controlling the tacticity of the final products, the ability to control the polymer topology is limited. The latest effort in this regard describes the use of intramolecular hydrogen bonding to shorten the intervinylic distance of DVMs, facilitating the cyclopolymerization, as achieved in the oligo(ethylene glycol) bisacrylamide (OEG<sub>n</sub>DAAm, *n* = 3–6, Figure 5, **15**).<sup>108</sup>

The formation of pseudo-crown ether structures by complexation of ether oxygens in ethylene glycol based divinyl monomers to a cation has been used to shorten the end-to-end distance and enhance cyclopolymerization.<sup>109</sup> In a recent study (Box 2b), such cation templated oligo(ethylene glycol) dimethacrylate (OEG<sub>n</sub>DMA, *n* = 4, 5, 6, 8) with pseudo-cyclic conformation was successfully cyclopolymerized by ruthenium mediated RDRP under high dilution (0.025 – 0.1 M), yielding soluble polymers with well-defined MW, large pendent poly(ethylene glycol) (PEG) rings (19- to 30-membered rings) and low dispersity at high conversion (~90%).<sup>110</sup> The average intervinylic distance in OEG<sub>6</sub>DMA was efficiently reduced to 4.7 Å with the addition of KPF<sub>6</sub>, which is in line with the “5 Å rule”. The metal–ligand coordination chemistry was also used to generate oriented pseudo DVMs for cyclopolymerization, producing main-chain chiral polymers<sup>111</sup> or sequence-regulated polymers.<sup>112</sup>

**[H3] Polymerization in coordination nanochannels.** Using functional molecular-scale spaces, such as crystals, mesoporous silicas/aluminas, and metal-organic frameworks, to control the polymerization process and regulate the resulting polymer structure, is a new avenue of research in polymer science.<sup>113</sup> Uemura and Kitagawa successfully applied this technique to MVM polymerization, achieving a selective linear polymerization<sup>114</sup> or cyclopolymerization<sup>115</sup> of DVMs in 1D nanochannels. An essential requirement for such polymerization is to select an channel of appropriate size for the guest monomers: no polymerization occurred when the nanoscale channels were too small, and insoluble crosslinked structures are resulted when channels were too large.<sup>114</sup> As shown in Figure 5c, the authors demonstrated that controlled radical cyclopolymerization of 1,6-diene-type monomers could be achieved in such 1D nanochannels of [Cu<sub>2</sub>(L)<sub>2</sub>(dabco)]<sub>n</sub> (L = dicarboxylates, dabco = 1,4-diazabicyclo[2.2.2]octane).<sup>115</sup> For the

polymerization of acrylic anhydride, six-membered anhydride rings were dominantly formed, suggesting that formation of the cyclic structure might be finely regulated in these nanochannels.

### *[H2] Single-chain cyclized polymers*

Single-chain cyclized polymers are the result of a coexisting intra-chain cyclization and chain propagation synthesis process and feature a highly looped single chain topology. The general synthesis process of a single-chain cyclized polymer from DE-ATRP of MVMs is illustrated in Box 3. At the initial stage, in a fashion similar to linear RDRP reactions, monomer addition is expected to occur by reaction between an active radical with one vinyl group in a free monomer and leads to the formation of primary linear chains. This is consistent with the experimental results that show a linear increase of MW with increasing monomer conversion, and a low dispersity with a unimodal gel permeation chromatography peak. At this stage, the lower polymer volume concentration and the smaller growth boundary achieved by DE strategy, act collectively to reduce the likelihood of the polymer chains from reacting with the pendent vinyl groups of other growing polymer chains. Consequently, only the monomeric and same-chain pendent vinyl groups are able to be polymerized by the propagating center. The addition of monomeric vinyl groups results in linear chain propagation and the generation of pendent vinyl groups simultaneously. The reactions between the chain end radicals (propagating centers) with the pendent vinyl groups located on that same primary chain result in the formation of lasso-like covalent loops in a closed ring manner. The radical formed at the end of the lasso can further participate in the polymerization either by monomer addition or by further intramolecular cyclization. It has been difficult to experimentally detect the emerging moment of intramolecular cyclization, however, according to <sup>1</sup>H-NMR spectroscopic studies, 28.3% of the pendent vinyl groups were consumed after only 8.3% monomer conversion during this linear chain growth phase.<sup>116</sup> Given that the pendent vinyl conversion at zero monomer conversion indicates the extent of intramolecular cyclization,<sup>117</sup> a large amount of pendent vinyls have been cyclized, resulting in multiple cyclic units within the newly born primary chain. It should be noted here however, that in comparison to cyclopolymers, the single-chain cyclized polymers feature incomplete cyclization, i.e., the existence of the unreacted pendent vinyl groups. These unreacted pendent vinyl groups, located in the newly formed loops can further participate in the chain growth, leading to loop-loop connection and a covalent knot structure, as found in proteins.<sup>118</sup> Therefore, the products isolated at this stage are termed as single-chain cyclized polymers, and show a globular morphology from Atomic Force Microscopy (AFM) with low dispersity and a **Mark-Houwink exponent ( $\alpha$ ) [G]** of  $\sim 0.3$ , supporting the spherical molecular conformation.<sup>116</sup>

The presence of intra-chain crosslinkages was further confirmed by comparing the molecular weight of the degraded products with the non-degraded one. By placing a cleavable spacer between the two vinyl groups<sup>116,119</sup>, one can collect and analyze the primary chains after subjecting the polymer to conditions that will degrade the cleavable monomer. Such uncoupling of single-chain cyclized polymers results in a minimum change in MW, as the cleavable linkers are located at either pendent chains or intra-chain loops. The cleavage of the linker only removes the dangling parts and breaks the loops, leaving the nondegradable primary chain unchanged. Such a degradation process can be viewed as an untying process of the cyclized and knotted units.<sup>59,116,119</sup> In contrast, however, using similar cleavable divinyl monomers to form branched polymers comprising of short primary chains, where the degradable linkage lies between

chains (inter-chain linkers), show a different uncoupling profile. In this situation, the subsequent degradation generates smaller fragments of polymer chains with a significant decrease in MW.<sup>55,120</sup>

### [H1] Characterization of chain connections

The advancement of architecturally complex polymer synthesis is often challenged by the lack of proper characterization techniques, leaving polymer architectures that are too complex for traditional polymer analytics. This is particularly true when attempting to distinguish and quantify inter-chain and intra-chain linkages, which are chemically and spectroscopically similar. Although conventional characterization strategies tend to be indirect, direct characterization methods such as the determination of intra-chain linkages based on the <sup>1</sup>H-NMR spectroscopy reported by Armes and coworkers<sup>121</sup> do have some potential. Studying the FRP of methyl methacrylate (MMA) with disulfide-based dimethacrylate, they observed higher frequency chemical shifts for thiamethylene (S–S–CH<sub>2</sub>) protons in cyclic linkages than linear chain linkages ( $\delta$  3.00 ppm vs.  $\delta$  2.92 ppm), (Figure 6a). The difference in chemical environment between the cyclic and noncyclic linkages was attributed to the gauche effect arising from the 90° dihedral angle of disulfide bonds, but this difference was only sufficient to resolve the signals in small cycles, limiting the applicability of this method.

An outstanding strategy for quantifying intra-chain connections, termed symmetric isotopic labelling disassembly spectrometry (SILDaS), was recently developed by Johnson and coworkers, represents the first direct, precise, and model-free loop quantification technique.<sup>122–124</sup> The technique was originally proposed for the analysis of endlinked polymer networks and was more recently extended to sidechain-crosslinked polymers.<sup>125</sup> The method relies on the synthesis of polymer networks using cleavable and isotope-labelled precursors, and the topological information (for example, the number of intra-chain crosslinks) can be reconstructed by quantifying the different types of degradation fragments using liquid chromatography–mass spectrometry (LC-MS) as shown in Figure 6b. In the case of sidechain-crosslinked polymers, a known ratio of deuterium-labelled and unlabelled primary chains were mixed and crosslinked. When the polymer network is later degraded, by cleavage of a pendent ester, the ratio of intra-chain to inter-chain connections can be determined by quantifying the mass distribution of unlabelled, half-labelled and fully labelled degradation products. To best of our knowledge, the direct application of this technique to characterize the crosslinkages in MVM-derived polymers has not yet been reported. But it holds the most promise in accurately characterizing and quantifying the inter-chain and intra-chain connections. This is of fundamental interest for elucidating structure–property relationships, an essential component in the development of advanced polymer materials from such architecturally intricate macromolecules.

For polymers with complex architectures, the sample averaged set of analytical data is typically unable to capture fully the structure features. Thus single molecule characterization strategies are highly desirable to probe both the structural homogeneity or the unique micromechanics.<sup>126</sup> Recent advances in single-molecule imaging and spectroscopy techniques— typically designed originally for the analysis of biomacromolecules such as proteins and nucleic acids,<sup>127,128</sup> — have also opened new avenues for the characterization, visualization and manipulation of architecturally complex polymers. Atomic force microscopy (AFM) has been successfully applied to visualize individual polymer

molecules, such as the individual star-like polymer architecture, to illustrate their overall morphology or coil/globular chain features.<sup>129</sup> However, this technique is limited to large and stiff polymers and is thus not widely applicable to most synthetic polymers, and it remains extremely challenging to directly visualize the sub-chain connections.

Aside from imaging, AFM also enables the evaluation of a variety of polymer physical properties, which are closely correlated to their subchain connections, such as the elasticity<sup>126</sup> and conductance.<sup>130</sup> Remarkably, after decades of development, AFM based single-molecule force spectroscopy (SMFS) has been demonstrated to be capable of probing the conformational changes occurring in an individual molecule level when stretching a polymer chain to the point of bond rupture.<sup>127,131</sup> The inherent structural differences between intra- and inter-chain crosslinkings would mean that mechanically breaking the first would lead to chain elongation while breaking the second will lead to chain rupture. This concept has been verified successfully in protein unfolding research where intra-chain disulfide bridges were cleaved by the addition of thiol<sup>132,133</sup> or hydroxide nucleophiles<sup>134</sup> under stretching. Such rupture events are marked by chain elongations that correspond to the folded chain length behind the disulfide bond (Figure 6c).<sup>134</sup> In a recent report, mechanical unfolding of synthetic polymers with multiple intra-chain hydrogen bonding was described by Meijer and coworkers.<sup>135</sup> The contour length, and the number of the rupture events as collected from the consecutive force peaks, were used to correlate the amount of intra-chain linkages (Figure 6d). This example and others<sup>136–138</sup> illustrate the feasibility and relevance of mechanically unfolding polymers for the characterization of sub-chain connections.

### **[H1] Emerging biomedical applications**

With the ability to tailor complex polymer architectures on a molecular level, free radical polymerization of MVMs provides a good platform to develop advanced functional polymers. Architecturally complex polymers, built from biocompatible, biodegradable and functionalizable molecules, can serve as innovative building blocks for the development of cutting-edge biomaterials, showing superior performance over their linear counterparts.<sup>139</sup> Furthermore, inspiration for complex architecture achieved through MVM polymerization can be gleaned from the delicate biofunctions of naturally existing biomacromolecules such as circular plasmids, branched glycogens/polysaccharides or nucleic acids with in-chain multiple cyclic units. A notable example is DIVEMA (pyran copolymer), synthesized by free radical cyclopolymerization of divinyl ether and maleic anhydride.<sup>140</sup> It is known as the first clinically tested polymeric anticancer agent with ability to induce interferon and activate immunocompetent cells.<sup>141</sup> An exemplary application of MVM derived polymers is as polymeric gene delivery vectors, where polymer architectures play a crucial role in dictating the physicochemical and biophysical properties of the polyplexes, and ultimately the overall gene transfection performance.<sup>142</sup> Cyclic polymers, due to their unique architectural characteristics (e.g., compact conformation and high charge density), manifest advantageous properties in gene delivery such as reduced cytotoxicity and prolonged circulation time *in vivo*, as demonstrated for cyclic Poly(dimethylaminoethyl methacrylate) (PDMAEMA)<sup>143</sup> and poly(ethylenimine).<sup>144</sup> Newland and co-workers have explored polyplex formation between single-chain cyclized polymers and plasmid DNA, revealing that the single-chain cyclized structure endows the polymers with the capability of condensing DNA in a loose conformation<sup>145</sup>

leading, in turn, to more efficient transfection and decreased cytotoxicity over the commercial reagent SuperFect (Figure 7).<sup>9,145</sup> Star and branched polymers also display similar topological effects that benefit their use in gene transfection.<sup>146,147</sup> For example, star shaped PDMAEMA has a strong buffering ability and the formulated polyplexes exhibited a loose morphology, which led to a superior gene transfection performance over their linear counterparts.<sup>148</sup> The introduction of degradable branching points into a high molecular weight PDMAEMA, has been shown to overcome the long-standing, and problematic, correlation between transfection efficacy and toxicity<sup>149</sup>

Similar topological effects have also been observed in other biomedical applications of polymers.<sup>150,151</sup> Bacterial contamination on medical device surfaces is a major safety issue in hospitals. Single-chain cyclized polymers were used to fabricate coatings which suppressed the formation of a biofilm. The nanoparticulate single-chain cyclized structure altered the surface morphology and hydrophobicity of the coatings, causing a reduction in bacterial attachment/biofilm formation of up to 75%, in comparison with traditional coatings prepared from FRP of MVMs.<sup>152</sup> Boyer and coworkers found, owning comparable antimicrobial activity, hyperbranched polymers have substantial better hemocompatibility comparing to the linear ones.<sup>153</sup>

Hyperbranched polymers have also been synthesized to overcome the poor sensitivity in traditional <sup>19</sup>F MRI caused by poor molecular mobility, association of the fluorinated segments and low fluorine content. The “shape-persistence” of hyperbranched structures enabled a high molecular mobility and fluorine content, which led the polymers to exhibit a high <sup>19</sup>F MRI sensitivity with the possibility of acquiring images within short acquisition times *in vivo*.<sup>154</sup> These encouraging results highlight that manipulation of polymer architecture by the controlled polymerization of MVMs provides a new way to enhance their diverse biomedical performance.

Another structural feature of MVM-derived polymers is the multiple residual vinyl groups, which can be further modified or crosslinked through diverse chemistries, such as photocrosslinking<sup>155</sup> or click chemistry<sup>156</sup>. In one example, the multiple pendant vinyl groups on a hyperbranched polymer from homopolymerized PEG diacrylate were modified with *N*-hydroxysuccinimide (NHS) groups to yield a crosslinkable, hyperbranched PEG-NHS polymer with over 12 NHS groups per molecule.<sup>157</sup> Such hyperbranched PEG diacrylate polymers could react with thiolated gelatin, forming a crosslinked hydrogel within minutes, due to the high content of residual vinyl groups.<sup>156</sup> Owing to the ease of structural manipulation, hydrogels from such systems are highly desired for manipulating cell behavior,<sup>158</sup> and are thus under extensive investigation for cell therapy<sup>156</sup>. Zhao and co-workers demonstrated the utility of single-chain cyclized polymers for fabricating injectable hydrogels for 3D cell encapsulation and showed that rapid crosslinking promoted long-term cell survival and proliferation.<sup>159</sup>

Besides these topological and structural effects, MVMs are also widely used as crosslinkers to hold the functional groups in position and/or maintain the configuration/morphology of polymeric materials. This function plays a critical role in their applications as biomaterials, such as in stem cell maintenance, self-renewal, directed differentiation, cell adhesion and harvesting, molecular recognition, adsorption, separation, and bacterial resistance.<sup>160–168</sup> For example, acid-degradable glycerol dimethacrylate was used to crosslink single-siRNA or protein nanocapsules by FRP, which can effectively protect cargos from enzymatic degradation and then release them in a triggered manner.<sup>169,170</sup> *N,N'*-methylenebisacrylamide (BIS) was used to crosslink nanoparticles for use as abiotic protein affinity reagents for

vascular endothelial growth factor (VEGF<sub>1650</sub>).<sup>171</sup> Another emerging application of MVMs as crosslinkers is for the construction of hydrogels used for expansion microscopy (ExM).<sup>15</sup> In a typical protocol, sodium acrylate, acrylamide and BIS are infused into fixed and permeabilized tissue samples and then polymerized to form a hydrogel *in situ*. After treatment with a protease, the tissue–polymer composite was dialyzed against water. Due to the strong isotropic swellability of the hydrogels, a 4.5-fold linear expansion of the specimen without distortion at the level of gross anatomy was achieved, which enabled super-resolution imaging on a conventional fluorescent microscope (Figure 8). The ExM technology further demonstrated its applicability in imaging human clinical specimens, visualization of RNA and proteins.<sup>172–174</sup>

It is worth noting that MVM derived polymers, when compared to dendrimers, bottlebrush and cyclic brush polymers, have some superiorities for biological/biomedical applications, such as broad monomer availability, ease of polymer synthesis, high structural flexibility and functionalizability. However, some limitations are yet to be overcome such as the relatively low monomer conversion for the synthesis of cyclized polymers; the broad molecular weight distribution of branched polymers, and the residual vinyl groups in polymers which can lead to gelation during storage.

## 6 Conclusions

Although the studies of FRP of MVMs have been conducted since the beginnings of polymer chemistry, recent advances in polymer science have led to exciting developments in the area. Unlike the traditional FRP of monovinyl monomers, the unique reaction kinetics and multiple potential propagation pathways of FRP of MVMs provide great flexibility in manipulating the chain topology and functionality. This results from the generation of polymerizable pendent vinyl moieties on the growing chains, enabling concurrent inter-chain combination and intra-chain cyclization. This increased tunability enables unprecedented control over the competing chain propagation events. This is assisted by the elaborate design of special MVMs, the control of gel points and the manipulation of the special distribution of crosslinking chain growth kinetics. These strategies have highlighted multivinyl radical polymerization as a highly efficient synthetic approach for the preparation of polymers with a variety of macromolecular architectures, including (hyper)branched, cyclopolymer, single-chain cyclized, star polymers and networks. The well-controlled structures and the inherent properties have stimulated many applications, especially in the biomedical area, ranging from therapeutic and diagnostic applications to tissue engineering. It can be envisaged that the continual development of synthetic approaches and an improved understanding of the structure–property relationships will facilitate further progress in the field.

However, despite the great progress achieved so far, multivinyl radical polymerization techniques still need to overcome several key challenges. A comprehensive understanding of the polymerization kinetics with concurrent chain growth, cyclization and crosslinking reactions has not yet been achieved. Complete control over the occurrence of competing propagation pathways remains challenging. Precise distinction and characterization of the inter-chain crosslinking units and intra-chain cyclization units in cyclic/branched/crosslinked polymers are outstanding issues that may be resolved with techniques such as network disassembly spectrometry. The formation of spatial inhomogeneity with fluctuations of concentration and crosslink density in the networks from multivinyl radical polymerization is not

yet fully understood and a theoretical framework that correlates such spatial inhomogeneity with mechanical properties (e.g. elasticity) is not yet available. Nevertheless, the versatile nature of multivinyl radical polymerization techniques make them a potentially efficient tool for achieving intricate structures, such as sequence-controlled or self-folding polymers. Moreover, the newly emerging applications (e.g. expansion microscopy and antimicrobial materials) will surely stimulate further development of this technique. Based on the large volume of work already reported and their future potential, we believe that multivinyl radical polymerization will continue generate new and innovative polymeric materials.

## References

1. PlasticsEurope. *Plastics - the Facts 2018*. (2018).
2. Nesvadba, P. in *Encyclopedia of Radicals in Chemistry, Biology and Materials* (John Wiley & Sons, Ltd, 2012). doi:10.1002/9781119953678.rad080
3. Matyjaszewski, K., Tsarevsky, N. V. Nanostructured functional materials prepared by atom transfer radical polymerization. *Nat. Chem.* **1**, 276–288 (2009).
4. Matyjaszewski, K. Chemistry. Architecturally complex polymers with controlled heterogeneity. *Science* **333**, 1104–1105 (2011).
5. Georges, M. K., Veregin, R. P. N., Kazmaier, P. M., Hamer, G. K. Narrow molecular weight resins by a free-radical polymerization process. *Macromolecules* **26**, 2987–2988 (1993).
6. Wang, J.-S., Matyjaszewski, K. Controlled/"living" radical polymerization. atom transfer radical polymerization in the presence of transition-metal complexes. *J. Am. Chem. Soc.* **117**, 5614–5615 (1995).
7. Chiefari, J., Chong, Y. K. (Bill), Ercole, F., Krstina, J., Jeffery, J., Le, T. P. T., Mayadunne, R. T. A., Meijs, G. F., Moad, C. L., Moad, G., Rizzardo, E., Thang, S. H. Living Free-Radical Polymerization by Reversible Addition–Fragmentation Chain Transfer: The RAFT Process. *Macromolecules* **31**, 5559–5562 (1998).
8. Stals, P. J. M., Li, Y., Burdyńska, J., Nicolaÿ, R., Nese, A., Palmans, A. R. a, Meijer, E. W., Matyjaszewski, K., Sheiko, S. S. How far can we push polymer architectures? *J. Am. Chem. Soc.* **135**, 11421–11424 (2013).
9. Newland, B., Zheng, Y., Jin, Y., Abu-Rub, M., Cao, H., Wang, W., Pandit, A. Single Cyclized Molecule Versus Single Branched Molecule: A Simple and Efficient 3D “Knot” Polymer Structure for Nonviral Gene Delivery. *J. Am. Chem. Soc.* **134**, 4782–4789 (2012).
10. Yang, C., Tibbitt, M. W., Basta, L., Anseth, K. S. Mechanical memory and dosing influence stem cell fate. *Nat. Mater.* **13**, 645–52 (2014).
11. Terashima, T., Kamigaito, M., Baek, K.-Y., Ando, T., Sawamoto, M. Polymer Catalysts from Polymerization Catalysts: Direct Encapsulation of Metal Catalyst into Star Polymer Core during Metal-Catalyzed Living Radical Polymerization. *J. Am. Chem. Soc.* **125**, 5288–5289 (2003).
12. Staudinger, H., Husemann, E. Über hochpolymere Verbindungen, 116. Mitteil.: Über das begrenzt quellbare Poly-styrol. *Berichte der Dtsch. Chem. Gesellschaft (A B Ser.)* **68**, 1618–1634 (1935).
13. Flory, P. J., Flory, J. Molecular Size Distribution in Three Dimensional Polymers. I. Gelation 1. *J. Am. Chem. Soc.* **63**, 3083–3090 (1941).



14. Stockmayer, W. H. Theory of Molecular Size Distribution and Gel Formation in Branched Polymers II. General Cross Linking. *J. Chem. Phys.* **12**, 125–131 (1944).
15. Chen, F. F., Tillberg, P. W., Boyden, E. S. Expansion microscopy. *Science* **347**, 543–548 (2015).  
**This work shows the application of free radical copolymerization of monovinyl/divinyl monomers for biological imaging.**
16. Distefano, G., Suzuki, H., Tsujimoto, M., Isoda, S., Bracco, S., Comotti, A., Sozzani, P., Uemura, T., Kitagawa, S. Highly ordered alignment of a vinyl polymer by host–guest cross-polymerization. *Nat. Chem.* **5**, 335–341 (2013).  
**This work describes the free radical copolymerization of monovinyl/divinyl monomers in porous coordination polymers, yielding a pseudo-crystalline polymeric network.**
17. Gu, Y., Zhao, J., Johnson, J. A. A (Macro)Molecular-Level Understanding of Polymer Network Topology. *Trends Chem.* **1**, 318–334 (2019).
18. Seiffert, S. Origin of nanostructural inhomogeneity in polymer-network gels. *Polym. Chem.* **8**, 4472–4487 (2017).
19. Matsumoto, A., Miwa, Y., Inoue, S., Enomoto, T., Aota, H. Discussion of “Greatly Delayed Gelation from Theory in Free-Radical Cross-Linking Multivinyl Polymerization Accompanied by Microgel Formation” Based on Multiallyl Polymerization. *Macromolecules* **43**, 6834–6842 (2010).
20. Okay, O., Kurz, M., Lutz, K., Funke, W. Cyclization and Reduced Pendant Vinyl Group Reactivity during the Free-Radical Cross-Linking Polymerization of 1,4-Divinylbenzene. *Macromolecules* **28**, 2728–2737 (1995).
21. Norisuye, T., Masui, N., Kida, Y., Ikuta, D., Kokufuta, E., Ito, S., Panyukov, S., Shibayama, M. Small angle neutron scattering studies on structural inhomogeneities in polymer gels: irradiation cross-linked gels vs chemically cross-linked gels. *Polymer* **43**, 5289–5297 (2002).
22. Adibnia, V., Hill, R. J. Universal aspects of hydrogel gelation kinetics, percolation and viscoelasticity from PA-hydrogel rheology. *J. Rheol.* **60**, 541–548 (2016).
23. Polanowski, P., Jeszka, J. K., Li, W., Matyjaszewski, K. Effect of dilution on branching and gelation in living copolymerization of monomer and divinyl cross-linker: Modeling using dynamic lattice liquid model (DLL) and Flory–Stockmayer (FS) model. *Polymer* **52**, 5092–5101 (2011).
24. Lyu, J., Gao, Y., Zhang, Z., Greiser, U., Polanowski, P., Jeszka, J. K., Matyjaszewski, K., Tai, H., Wang, W. Monte Carlo Simulations of Atom Transfer Radical (Homo)polymerization of Divinyl Monomers: Applicability of Flory–Stockmayer Theory. *Macromolecules* **51**, 6673–6681 (2018).
25. Elliott, J. E., Anseth, J. W., Bowman, C. N. Kinetic modeling of the effect of solvent concentration on primary cyclization during polymerization of multifunctional monomers. *Chem. Eng. Sci.* **56**, 3173–3184 (2001).
26. Cerid, H., Okay, O. Minimization of spatial inhomogeneity in polystyrene gels formed by free-radical mechanism. *Eur. Polym. J.* **40**, 579–587 (2004).
27. Elliott, J. E., Bowman, C. N. Effects of Solvent Quality during Polymerization on Network Structure of

- Cross-Linked Methacrylate Copolymers. *J. Phys. Chem. B* **106**, 2843–2847 (2002).
28. Doura, M., Naka, Y., Aota, H., Matsumoto, A. Control of Intermolecular Cross-Linking Reaction in Free-Radical Cross-Linking Monovinyl/Divinyl Copolymerizations by the Aid of Amphiphilic Nature of Primary Polymer Chains and Cross-Link Units with Opposite Polarities. *Macromolecules* **38**, 5955–5963 (2005).
  29. Mori, H., Tsukamoto, M. RAFT polymerization of diacrylate derivatives having different spacers in dilute conditions. *Polymer* **52**, 635–645 (2011).
  30. Yu, Q., Zhu, Y., Ding, Y., Zhu, S. Reaction Behavior and Network Development in RAFT Radical Polymerization of Dimethacrylates. *Macromol. Chem. Phys.* **209**, 551–556 (2008).
  31. Van Camp, W., Gao, H., Du Prez, F. E., Matyjaszewski, K. Effect of crosslinker multiplicity on the gel point in ATRP. *J. Polym. Sci. Part A Polym. Chem.* **48**, 2016–2023 (2010).
  32. Elliott, J. E., Bowman, C. N. Monomer Functionality and Polymer Network Formation. *Macromolecules* **34**, 4642–4649 (2001).
  33. Patras, G., Qiao, G. G., Solomon, D. H. Novel cross-linked homogeneous polyacrylamide gels with improved separation properties: Investigation of the cross-linker functionality. *Electrophoresis* **22**, 4303–4310 (2001).
  34. Denisin, A. K., Pruitt, B. L. Tuning the Range of Polyacrylamide Gel Stiffness for Mechanobiology Applications. *ACS Appl. Mater. Interfaces* **8**, 21893–21902 (2016).
  35. Shi, Y., Graff, R. W., Cao, X., Wang, X., Gao, H. Chain-Growth Click Polymerization of AB<sub>2</sub> Monomers for the Formation of Hyperbranched Polymers with Low Polydispersities in a One-Pot Process. *Angew. Chemie Int. Ed.* **54**, 7631–7635 (2015).
  36. O'Brien, N., McKee, A., Sherrington, D. C. C., Slark, A. T. T., Titterton, A. Facile, versatile and cost effective route to branched vinyl polymers. *Polymer* **41**, 6027–6031 (2000).
- This work proposes the “Strathclyde Route” for synthesizing branched polymers from radical polymerization of multivinyl monomers with the addition of chain transfer agents.**
37. Besenius, P., Slavin, S., Vilela, F., Sherrington, D. C. Synthesis and characterization of water-soluble densely branched glycopolymers. *React. Funct. Polym.* **68**, 1524–1533 (2008).
  38. Baudry, R., Sherrington, D. C. Synthesis of Highly Branched Poly(methyl methacrylate)s Using the “Strathclyde Methodology” in Aqueous Emulsion. *Macromolecules* **39**, 1455–1460 (2006).
  39. Chisholm, M., Hudson, N., Kirtley, N., Vilela, F., Sherrington, D. C. Application of the “Strathclyde Route” to Branched Vinyl Polymers in Suspension Polymerization: Architectural, Thermal, and Rheological Characterization of the Derived Branched Products. *Macromolecules* **42**, 7745–7752 (2009).
  40. Xiang, L., Song, Y., Qiu, M., Su, Y. Synthesis of Branched Poly(butyl acrylate) Using the Strathclyde Method in Continuous-Flow Microreactors. *Ind. Eng. Chem. Res.* **58**, 21312–21322 (2019).
  41. Guan, Z. Control of Polymer Topology through Transition-Metal Catalysis: Synthesis of Hyperbranched Polymers by Cobalt-Mediated Free Radical Polymerization. *J. Am. Chem. Soc.* **124**, 5616–5617 (2002).
  42. McEwan, K. A., Haddleton, D. M. Combining catalytic chain transfer polymerisation (CCTP) and thio-Michael addition: enabling the synthesis of peripherally functionalised branched polymers. *Polym. Chem.* **2**,

- 1992 (2011).
43. Smeets, N. M. B. B. Amphiphilic hyperbranched polymers from the copolymerization of a vinyl and divinyl monomer: The potential of catalytic chain transfer polymerization. *Eur. Polym. J.* **49**, 2528–2544 (2013).
  44. Kurochkin, S. A., Silant'ev, M. A., Perepelitsyna, E. O., Grachev, V. P. Synthesis of branched polymers via radical copolymerization under oxygen inflow. *Eur. Polym. J.* **57**, 202–212 (2014).
  45. Hirano, T., Kamiike, R., Hsu, Y., Momose, H., Ute, K. Multivariate analysis of <sup>13</sup>C NMR spectra of branched copolymers prepared by initiator-fragment incorporation radical copolymerization of ethylene glycol dimethacrylate and tert-butyl methacrylate. *Polym. J.* **48**, 793–800 (2016).
  46. Liang, S., Li, X., Wang, W.-J. J., Li, B.-G. G., Zhu, S. Toward Understanding of Branching in RAFT Copolymerization of Methyl Methacrylate through a Cleavable Dimethacrylate. *Macromolecules* **49**, 752–759 (2016).
  47. Bannister, I., Billingham, N. C., Armes, S. P., Rannard, S. P., Findlay, P. Development of Branching in Living Radical Copolymerization of Vinyl and Divinyl Monomers. *Macromolecules* **39**, 7483–7492 (2006).
  48. Rosselgong, J., Armes, S. P., Barton, W., Price, D. Synthesis of Highly Branched Methacrylic Copolymers: Observation of Near-Ideal Behavior using RAFT Polymerization. *Macromolecules* **42**, 5919–5924 (2009).
  49. Bannister, I., Billingham, N. C., Armes, S. P. Monte Carlo modelling of living branching copolymerisation of monovinyl and divinyl monomers: comparison of simulated and experimental data for ATRP copolymerisation of methacrylic monomers. *Soft Matter* **5**, 3495 (2009).
  50. Bouhier, M.-H., Cormack, P. A. G., Graham, S., Sherrington, D. C. Synthesis of densely branched poly(methyl methacrylate)s via ATR copolymerization of methyl methacrylate and ethylene glycol dimethacrylate. *J. Polym. Sci. Part A Polym. Chem.* **45**, 2375–2386 (2007).
  51. Liu, B., Kazlauciusas, A., Guthrie, J. T., Perrier, S. One-Pot Hyperbranched Polymer Synthesis Mediated by Reversible Addition Fragmentation Chain Transfer (RAFT) Polymerization. *Macromolecules* **38**, 2131–2136 (2005).
  52. Gao, H., Min, K., Matyjaszewski, K. Determination of Gel Point during Atom Transfer Radical Copolymerization with Cross-Linker. *Macromolecules* **40**, 7763–7770 (2007).
  53. Yang, H., Wang, Z., Zheng, Y., Huang, W., Xue, X., Jiang, B. Synthesis of highly branched polymers by reversible complexation-mediated copolymerization of vinyl and divinyl monomers. *Polym. Chem.* **8**, 2137–2144 (2017).
  54. Flynn, S., Dwyer, A. B., Chambon, P., Rannard, S. Expanding the monomer scope of linear and branched vinyl polymerisations via copper-catalysed reversible-deactivation radical polymerisation of hydrophobic methacrylates using anhydrous alcohol solvents. *Polym. Chem.* **10**, 5103–5115 (2019).
  55. Rosselgong, J., Armes, S. P., Barton, W. R. S., Price, D. Synthesis of Branched Methacrylic Copolymers: Comparison between RAFT and ATRP and Effect of Varying the Monomer Concentration. *Macromolecules* **43**, 2145–2156 (2010).
  56. Gao, Y., Newland, B., Zhou, D., Matyjaszewski, K., Wang, W. Controlled Polymerization of Multivinyl Monomers: Formation of Cyclized/Knotted Single-Chain Polymer Architectures. *Angew. Chemie Int. Ed.*

- 56**, 450–460 (2017).
57. Wang, W., Zheng, Y., Roberts, E., Duxbury, C. J., Ding, L., Irvine, D. J., Howdle, S. M. Controlling chain growth: A new strategy to hyperbranched materials. *Macromolecules* **40**, 7184–7194 (2007).
58. Zhao, T., Zhang, H., Zhou, D., Gao, Y., Dong, Y., Greiser, U., Tai, H., Wang, W. Water soluble hyperbranched polymers from controlled radical homopolymerization of PEG diacrylate. *RSC Adv.* **5**, 33823–33830 (2015).
59. Zhao, T., Zheng, Y., Poly, J., Wang, W. Controlled multi-vinyl monomer homopolymerization through vinyl oligomer combination as a universal approach to hyperbranched architectures. *Nat. Commun.* **4**, 1873 (2013).
- This work describes an universal approach to synthesize hyperbranched polymers from kinetically controlled multivinyl monomers.**
60. Odian, G. *Principles of Polymerization*. (Wiley, 2004).
61. Gao, H., Miasnikova, A., Matyjaszewski, K. Effect of Cross-Linker Reactivity on Experimental Gel Points during ATRcP of Monomer and Cross-Linker. *Macromolecules* **41**, 7843–7849 (2008).
62. Nagelsdiek, R., Mennicken, M., Maier, B., Keul, H., Höcker, H. Synthesis of Polymers Containing Cross-Linkable Groups by Atom Transfer Radical Polymerization: Poly(allyl methacrylate) and Copolymers of Allyl Methacrylate and Styrene. *Macromolecules* **37**, 8923–8932 (2004).
63. Yhaya, F., Sutinah, A., Gregory, A. M., Liang, M., Stenzel, M. H. RAFT polymerization of vinyl methacrylate and subsequent conjugation via enzymatic thiol-ene chemistry. *J. Polym. Sci. Part A Polym. Chem.* **50**, 4085–4093 (2012).
64. Akiyama, M., Yoshida, K., Mori, H. Controlled synthesis of vinyl-functionalized homopolymers and block copolymers by RAFT polymerization of vinyl methacrylate. *Polymer* **55**, 813–823 (2014).
65. Ma, J., Cheng, C., Sun, G., Wooley, K. L., Jun, M., Cheng, C., Sun, G., Wooley, K. L. Well-Defined Polymers Bearing Pendent Alkene Functionalities via Selective RAFT Polymerization. *Macromolecules* **41**, 9080–9089 (2008).
66. Ma, J., Cheng, C., Wooley, K. L. Cycloalkenyl-Functionalized Polymers and Block Copolymers: Syntheses via Selective RAFT Polymerizations and Demonstration of Their Versatile Reactivity. *Macromolecules* **42**, 1565–1573 (2009).
67. Qu, Q., Liu, G., Lv, X., Zhang, B., An, Z. In Situ Cross-Linking of Vesicles in Polymerization-Induced Self-Assembly. *ACS Macro Lett.* **5**, 316–320 (2016).
68. Chen, L., Li, Y., Yue, S., Ling, J., Ni, X., Shen, Z. Chemoselective RAFT Polymerization of a Trivinyl Monomer Derived from Carbon Dioxide and 1,3-Butadiene: From Linear to Hyperbranched. *Macromolecules* [acs.macromol.7b02238](https://doi.org/10.1021/acs.macromol.7b02238) (2017). doi:10.1021/acs.macromol.7b02238
69. Dong, Z. M., Liu, X. H., Tang, X. L., Li, Y. S. Synthesis of Hyperbranched Polymers with Pendent Norbornene Functionalities via RAFT Polymerization of a Novel Asymmetrical Divinyl Monomer. *Macromolecules* **42**, 4596–4603 (2009).
70. Ren, J. M., McKenzie, T. G., Fu, Q., Wong, E. H. H., Xu, J., An, Z., Shanmugam, S., Davis, T. P., Boyer,

- C., Qiao, G. G. Star Polymers. *Chem. Rev.* **116**, 6743–6836 (2016).
71. Gao, H., Matyjaszewski, K. Synthesis of functional polymers with controlled architecture by CRP of monomers in the presence of cross-linkers: From stars to gels. *Prog. Polym. Sci.* **34**, 317–350 (2009).
72. Wang, D., Li, X., Wang, W. J., Gong, X., Li, B. G., Zhu, S. Kinetics and modeling of semi-batch RAFT copolymerization with hyperbranching. *Macromolecules* **45**, 28–38 (2012).
- This work describes the synthesis of branched polymers from semi-batch copolymerization of multivinyl monomers.**
73. Wang, D., Wang, W.-J., Li, B.-G., Zhu, S. Semibatch RAFT polymerization for branched polyacrylamide production: Effect of divinyl monomer feeding policies. *AIChE J.* **59**, 1322–1333 (2013).
74. Xia, J., Zhang, X., Matyjaszewski, K. Synthesis of star-shaped polystyrene by atom transfer radical polymerization using an ‘arm first’ approach. *Macromolecules* **32**, 4482–4484 (1999).
75. Gao, H., Matyjaszewski, K. Synthesis of Miktoarm Star Polymers via ATRP Using the “In–Out” Method: Determination of Initiation Efficiency of Star Macroinitiators. *Macromolecules* **39**, 7216–7223 (2006).
76. Connal, L. A., Vestberg, R., Hawker, C. J., Qiao, G. G., Connal, L. A., Vestberg, R., Hawker, C. J., Qiao, G. G. Synthesis of Dendron Functionalized Core Cross-linked Star Polymers. *Macromolecules* **40**, 7855–7863 (2007).
77. Hatton, F. L., Chambon, P., McDonald, T. O., Owen, A., Rannard, S. P. Hyperbranched polydendrons: a new controlled macromolecular architecture with self-assembly in water and organic solvents. *Chem. Sci.* **5**, 1844–1853 (2014).
78. Hern, F. Y., Hill, A., Owen, A., Rannard, S. P. Co-initiated hyperbranched-polydendron building blocks for the direct nanoprecipitation of dendron-directed patchy particles with heterogeneous surface functionality. *Polym. Chem.* **9**, 1767–1771 (2018).
79. Kanaoka, S., Sawamoto, M., Higashimura, T. Star-shaped polymers by living cationic polymerization. 1. Synthesis of star-shaped polymers of alkyl and vinyl ethers. *Macromolecules* **24**, 2309–2313 (1991).
80. Gao, H., Matyjaszewski, K. Structural Control in ATRP Synthesis of Star Polymers Using the Arm-First Method. *Macromolecules* **39**, 3154–3160 (2006).
81. Baek, K.-Y. Y., Kamigaito, M., Sawamoto, M. Star-shaped polymers by metal-catalyzed living radical polymerization. 1. Design of Ru(II)-based systems and divinyl linking agents. *Macromolecules* **34**, 215–221 (2001).
82. Baek, K.-Y., Kamigaito, M., Sawamoto, M. Core-Functionalized Star Polymers by Transition Metal-Catalyzed Living Radical Polymerization. 1. Synthesis and Characterization of Star Polymers with PMMA Arms and Amide Cores 1. *Macromolecules* **34**, 7629–7635 (2001).
83. Li, W., Matyjaszewski, K. Star Polymers via Cross-Linking Amphiphilic Macroinitiators by AGET ATRP in Aqueous Media. *J. Am. Chem. Soc.* **131**, 10378–10379 (2009).
84. Zhang, X., Xia, J., Matyjaszewski, K. End-Functional Poly(tert-butyl acrylate) Star Polymers by Controlled Radical Polymerization. *Macromolecules* **33**, 2340–2345 (2000).
85. Pasquale, A. J., Long, T. E. Synthesis of star-shaped polystyrenes via nitroxide-mediated stable free-radical

- polymerization. *J. Polym. Sci. Part A Polym. Chem.* **39**, 216–223 (2001).
86. Gao, H., Matyjaszewski, K. Synthesis of Star Polymers by A New “Core-First” Method: Sequential Polymerization of Cross-Linker and Monomer. *Macromolecules* **41**, 1118–1125 (2008).
  87. Butler, G. B., Bunch, R. L. Preparation and Polymerization of Unsaturated Quaternary Ammonium Compounds. *J. Am. Chem. Soc.* **71**, 3120–3122 (1949).
  88. Butler, G. B., Ingley, F. L. Preparation and Polymerization of Unsaturated Quaternary Ammonium Compounds. II. Halogenated Allyl Derivatives 1,2. *J. Am. Chem. Soc.* **73**, 895–896 (1951).
  89. Pasini, D., Takeuchi, D. Cyclopolymerizations: Synthetic Tools for the Precision Synthesis of Macromolecular Architectures. *Chem. Rev.* **118**, 8983–9057 (2018).
  90. Matsumoto, A., Tanaka, T., Tsubouchi, T., Tashiro, K., Saragai, S., Nakamoto, S. Crystal Engineering for Topochemical Polymerization of Muconic Esters Using Halogen–Halogen and CH/ $\pi$  Interactions as Weak Intermolecular Interactions. *J. Am. Chem. Soc.* **124**, 8891–8902 (2002).
  91. Crawshaw, A., Butler, G. B. The Formation of Linear Polymers from Diene Monomers by a Cyclic Polymerization Mechanism. II. Polyacrylic Anhydride and the Derived Polyacrylic Acid 1,2. *J. Am. Chem. Soc.* **80**, 5464–5466 (1958).
  92. Tsukino, M., Kunitake, T. Radical Cyclopolymerization of Divinyl Acetals—Structure Variation with Polymerization Conditions. *Polym. J.* **17**, 943–951 (1985).
  93. Costa, L., Chiantore, O., Guaita, M. Free radical polymerization of unconjugated dienes: 19. Temperature dependence of the cyclopolymerization of o-divinylbenzene. *Polymer* **19**, 202–204 (1978).
  94. Jones, R. G., Harry Cragg, R., Swain, A. C. Structure and mechanism in the cyclopolymerization of diallylsilanes. *Eur. Polym. J.* **28**, 651–655 (1992).
  95. Erkoc, S., Mathias, L. J., Acar, A. E. Cyclopolymerization of tert -Butyl  $\alpha$ -(Hydroxymethyl) Acrylate (TBHMA) Ether Dimer via Atom Transfer Radical Polymerization (ATRP). *Macromolecules* **39**, 8936–8942 (2006).
  96. Erkoc, S., Acar, A. E. Controlled/Living Cyclopolymerization of tert -Butyl  $\alpha$ -(Hydroxymethyl) Acrylate Ether Dimer via Reversible Addition Fragmentation Chain Transfer Polymerization. *Macromolecules* **41**, 9019–9024 (2008).
  97. Yokota, K., Matsumura, M., Yamaguchi, K., Takada, Y. Synthesis of Polymers with Benzo-19-crown-6 Units via Cyclopolymerization of Divinyl Ethers Kazuaki. *Macromol. Rapid Commun.* **4**, 721–724 (1983).
  98. Wulff, G., Schmidt, H., Witt, H., Zentel, R. Cooperativity and Transfer of Chirality in Liquid-Crystalline Polymers. *Angew. Chemie Int. Ed. English* **33**, 188–191 (1994).
  99. Kakuchi, T., Narumi, A., Kaga, H., Yamauchi, Y., Obata, M., Uesaka, T., Yokota, K. Chirality Induction in Cyclopolymerization. 14. Template Effect of 1,2-Cycloalkanediol in the Cyclopolymerization of Bis(4-vinylbenzoate)s with Styrene. *Macromolecules* **34**, 38–43 (2001).
  100. Zhao, X., Liu, H. Synthesis and Characterization of PEG Polymer Brushes via Cyclopolymerization of 1,2,3-Triazole Tethered Diacrylates. *Chinese J. Chem. Phys.* **28**, 739–745 (2015).
  101. Ochiai, B., Shiomi, T., Yoshita, H. Cyclopolymerization of a bisacrylate through selective formation of a

- 19-membered ring. *Polym. J.* **48**, 859–862 (2016).
102. Ochiai, B., Ootani, Y., Endo, T. Controlled Cyclopolymerization through Quantitative 19-Membered Ring Formation. *J. Am. Chem. Soc.* **130**, 10832–10833 (2008).
103. Kim, T.-H., Feeder, N., Holmes, A. B., Dokolas, P., Giles, M., Walther, M. Cyclopolymerisation of an oriented 4,6-bis(4-vinylbenzyl)-myo-inositol orthoformate. *Chem. Commun.* 2419–2420 (2000). doi:10.1039/b007057m
104. Kim, T.-H., Holmes, A. B., Giles, M. Ring closing metathesis of a 4,6-diallyl-myoinositol orthoformate as a model for an inositol cyclopolymer. *Chem. Commun.* 2421–2422 (2000). doi:10.1039/b007058k
105. Li, J., Du, M., Zhao, Z., Liu, H. Cyclopolymerization of Disiloxane-Tethered Divinyl Monomers To Synthesize Chirality-Responsive Helical Polymers. *Macromolecules* **49**, 445–454 (2016).
106. Saito, Y., Saito, R. Synthesis of syndiotactic poly(methacrylic acid) by free-radical polymerization of the pseudo-divinyl monomer formed with methacrylic acid and catechol. *J. Appl. Polym. Sci.* **128**, 3528–3533 (2013).
107. Kang, Y., Lu, A., Ellington, A., Jewett, M. C., O'Reilly, R. K. Effect of Complementary Nucleobase Interactions on the Copolymer Composition of RAFT Copolymerizations. *ACS Macro Lett.* **2**, 581–586 (2013).
108. Kimura, Y., Miyabara, Y., Terashima, T., Sawamoto, M. Polyacrylamide pseudo crown ethers via hydrogen bond-assisted cyclopolymerization. *J. Polym. Sci. Part A Polym. Chem.* **54**, 3294–3302 (2016).
109. Mathur, A. M., Scranton, A. B. Synthesis and Ion-Binding Properties of Polymeric Pseudocrown Ethers II: Template Ion Induced Cyclization of Oligomeric Ethylene Glycol Diacrylates. *Sep. Sci. Technol.* **32**, 285–301 (1997).
110. Terashima, T., Kawabe, M., Miyabara, Y., Yoda, H., Sawamoto, M. Polymeric pseudo-crown ether for cation recognition via cation template-assisted cyclopolymerization. *Nat. Commun.* **4**, 2321 (2013).  
**This work presents the cyclopolymerization of divinyl monomers in the presence of cation template.**
111. Jana, S., Sherrington, D. C. Transfer of Chirality from (–)-Sparteine Zinc(II) (Meth)acrylate Complexes to the Main Chains of Their (Meth)acrylate Polymer Derivatives. *Angew. Chemie Int. Ed.* **44**, 4804–4808 (2005).
112. Hibi, Y., Ouchi, M., Sawamoto, M. Sequence-Regulated Radical Polymerization with a Metal-Templated Monomer: Repetitive ABA Sequence by Double Cyclopolymerization. *Angew. Chemie Int. Ed.* **50**, 7434–7437 (2011).  
**This work describes the synthesis of sequence-controlled polymers via cyclopolymerization of multivinyl monomers.**
113. Mochizuki, S., Kitao, T., Uemura, T. Controlled polymerizations using metal–organic frameworks. *Chem. Commun.* **54**, 11843–11856 (2018).
114. Uemura, T., Hiramatsu, D., Kubota, Y., Takata, M., Kitagawa, S. Topotactic Linear Radical Polymerization of Divinylbenzenes in Porous Coordination Polymers. *Angew. Chemie Int. Ed.* **46**, 4987–4990 (2007).

115. Nakanishi, R., Uemura, T., Kitagawa, S., Nakanishi, R., Kaseda, T., Uchida, N., Kitagawa, S. Controlled Cyclopolymerization of Difunctional Vinyl Monomers in Coordination Nanochannels. *Macromolecules* **47**, 7321–7326 (2014).
116. Gao, Y., Zhou, D., Zhao, T., Wei, X., McMahon, S., O’Keeffe Ahern, J., Wang, W., Greiser, U., Rodriguez, B. J., Wang, W. Intramolecular Cyclization Dominating Homopolymerization of Multivinyl Monomers toward Single-Chain Cyclized/Knotted Polymeric Nanoparticles. *Macromolecules* **48**, 6882–6889 (2015).
117. Elliott, J. E., Bowman, C. N. Kinetics of primary cyclization reactions in cross-linked polymers: An analytical and numerical approach to heterogeneity in network formation. *Macromolecules* **32**, 8621–8628 (1999).
118. Taylor, W. R., Lin, K. Protein knots: A tangled problem. *Nature* **421**, 25–25 (2003).
119. Zheng, Y., Cao, H. L., Newland, B., Dong, Y. X., Pandit, A., Wang, W. 3D single cyclized polymer chain structure from controlled polymerization of multi-vinyl monomers: Beyond Flory-Stockmayer theory. *J. Am. Chem. Soc.* **133**, 13130–13137 (2011).

**This work describes the synthesis of single cyclized polymers from intramolecular cyclization dominated polymerization of multivinyl monomers.**

120. Li, Y., Armes, S. P. Synthesis and Chemical Degradation of Branched Vinyl Polymers Prepared via ATRP: Use of a Cleavable Disulfide-Based Branching Agent. *Macromolecules* **38**, 8155–8162 (2005).
121. Rosselgong, J., Armes, S. P. Quantification of Intramolecular Cyclization in Branched Copolymers by <sup>1</sup>H NMR Spectroscopy. *Macromolecules* **45**, 2731–2737 (2012).
122. Zhou, H., Woo, J., Cok, A. M., Wang, M., Olsen, B. D., Johnson, J. A. Counting primary loops in polymer gels. *Proc. Natl. Acad. Sci.* **109**, 19119–19124 (2012).
123. Wang, J., Lin, T. S., Gu, Y., Wang, R., Olsen, B. D., Johnson, J. A. Counting Secondary Loops Is Required for Accurate Prediction of End-Linked Polymer Network Elasticity. *ACS Macro Lett.* **7**, 244–249 (2018).
124. Zhong, M., Wang, R., Kawamoto, K., Olsen, B. D., Johnson, J. A. Quantifying the impact of molecular defects on polymer network elasticity. *Science* **353**, 1264–1268 (2016).

**This work proposes a technique, called symmetric isotopic labeling disassembly spectrometry (SILDaS), to quantify the intra-chain links (loops) in polymer network.**

125. Wang, J., Wang, R., Gu, Y., Sourakov, A., Olsen, B. D., Johnson, J. A. Counting loops in sidechain-crosslinked polymers from elastic solids to single-chain nanoparticles. *Chem. Sci.* **10**, 5332–5337 (2019).
126. Wang, D., Russell, T. P. Advances in Atomic Force Microscopy for Probing Polymer Structure and Properties. *Macromolecules* **51**, 3–24 (2018).
127. Pavliček, N., Gross, L. Generation, manipulation and characterization of molecules by atomic force microscopy. *Nat. Rev. Chem.* **1**, 0005 (2017).
128. Krieg, M., Fläschner, G., Alsteens, D., Gaub, B. M., Roos, W. H., Wuite, G. J. L., Gaub, H. E., Gerber, C., Dufrêne, Y. F., Müller, D. J. Atomic force microscopy-based mechanobiology. *Nat. Rev. Phys.* **1**, 41–57 (2019).



129. Burdyńska, J., Li, Y., Aggarwal, A. V., Höger, S., Sheiko, S. S., Matyjaszewski, K. Synthesis and Arm Dissociation in Molecular Stars with a Spoked Wheel Core and Bottlebrush Arms. *J. Am. Chem. Soc.* **136**, 12762–12770 (2014).
130. Lafferentz, L., Ample, F., Yu, H., Hecht, S., Joachim, C., Grill, L. Conductance of a Single Conjugated Polymer as a Continuous Function of Its Length. *Science* **323**, 1193–1197 (2009).
131. Chung, J., Kushner, A. M., Weisman, A. C., Guan, Z. Direct correlation of single-molecule properties with bulk mechanical performance for the biomimetic design of polymers. *Nat. Mater.* **13**, 1055–1062 (2014).
132. Beedle, A. E. M., Mora, M., Davis, C. T., Snijders, A. P., Stirnemann, G., Garcia-Manyes, S. Forcing the reversibility of a mechanochemical reaction. *Nat. Commun.* **9**, 3155 (2018).
133. Wiita, A. P., Perez-Jimenez, R., Walther, K. A., Gräter, F., Berne, B. J., Holmgren, A., Sanchez-Ruiz, J. M., Fernandez, J. M. Probing the chemistry of thioredoxin catalysis with force. *Nature* **450**, 124–127 (2007).
134. Garcia-Manyes, S., Liang, J., Szoszkiewicz, R., Kuo, T.-L., Fernández, J. M. Force-activated reactivity switch in a bimolecular chemical reaction. *Nat. Chem.* **1**, 236–242 (2009).
135. Hosono, N., Kushner, A. M., Chung, J., Palmans, A. R. A., Guan, Z., Meijer, E. W. Forced unfolding of single-chain polymeric nanoparticles. *J. Am. Chem. Soc.* **137**, 6880–6888 (2015).
136. Levy, A., Feinstein, R., Diesendruck, C. E. Mechanical Unfolding and Thermal Refolding of Single-Chain Nanoparticles Using Ligand–Metal Bonds. *J. Am. Chem. Soc.* **141**, 7256–7260 (2019).
137. Liu, N., Zhang, W. Feeling Inter- or Intramolecular Interactions with the Polymer Chain as Probe: Recent Progress in SMFS Studies on Macromolecular Interactions. *ChemPhysChem* **13**, 2238–2256 (2012).
138. Huang, Z., Delparastan, P., Burch, P., Cheng, J., Cao, Y., Messersmith, P. B. Injectable dynamic covalent hydrogels of boronic acid polymers cross-linked by bioactive plant-derived polyphenols. *Biomater. Sci.* **6**, 2487–2495 (2018).
139. Kakkar, A., Traverso, G., Farokhzad, O. C., Weissleder, R., Langer, R. Evolution of macromolecular complexity in drug delivery systems. *Nat. Rev. Chem.* **1**, 0063 (2017).
140. BRESLOW, D. S., EDWARDS, E. I., NEWBURG, N. R. Divinyl Ether-Maleic Anhydride (Pyran) Copolymer used to demonstrate the Effect of Molecular Weight on Biological Activity. *Nature* **246**, 160–162 (1973).
141. Duncan, R. The dawning era of polymer therapeutics. *Nat. Rev. Drug Discov.* **2**, 347–60 (2003).
142. Zhou, D., Wang, W., Cutlar, L., Gao, Y., Wang, W., O’Keeffe-Ahern, J., McMahon, S., Greiser, U., Duarte, B., Larcher, F., Rodriguez, B. J. The transition from linear to highly branched poly( $\beta$ -amino ester)s: Branching matters for gene delivery. *Sci Adv* **2**, e1600102 (2016).
143. Wei, H., Chu, D. S. H., Zhao, J., Pahang, J. a., Pun, S. H. Synthesis and Evaluation of Cyclic Cationic Polymers for Nucleic Acid Delivery. *ACS Macro Lett.* **2**, 1047–1050 (2013).
144. Cortez, M. A., Godbey, W. T., Fang, Y., Payne, M. E., Cafferty, B. J., Kosakowska, K. A., Grayson, S. M. The Synthesis of Cyclic Poly(ethylene imine) and Exact Linear Analogues: An Evaluation of Gene Delivery Comparing Polymer Architectures. *J. Am. Chem. Soc.* **137**, 6541–6549 (2015).
145. Newland, B., Abu-Rub, M., Naughton, M., Zheng, Y., Pinoncely, A. V., Collin, E., Dowd, E., Wang, W.,

- Pandit, A. GDNF gene delivery via a 2-(dimethylamino)ethyl methacrylate based cyclized knot polymer for neuronal cell applications. *ACS Chem. Neurosci.* **4**, 540–546 (2013).
146. Cook, A. B., Peltier, R., Barlow, T. R., Tanaka, J., Burns, J. A., Perrier, S. Branched poly (trimethylphosphonium ethylacrylate- co -PEGA) by RAFT: alternative to cationic polyammoniums for nucleic acid complexation. *J. Interdiscip. Nanomedicine* **3**, 164–174 (2018).
147. Cho, H. Y., Srinivasan, A., Hong, J., Hsu, E., Liu, S., Shrivats, A., Kwak, D., Bohaty, A. K., Paik, H., Hollinger, J. O., Matyjaszewski, K. Synthesis of Biocompatible PEG-Based Star Polymers with Cationic and Degradable Core for siRNA Delivery. *Biomacromolecules* **12**, 3478–3486 (2011).
148. Dai, F., Sun, P., Liu, Y., Liu, W. Redox-cleavable star cationic PDMAEMA by arm-first approach of ATRP as a nonviral vector for gene delivery. *Biomaterials* **31**, 559–569 (2010).
149. Zhao, T., Zhang, H., Newland, B., Aied, A., Zhou, D., Wang, W. Significance of Branching for Transfection: Synthesis of Highly Branched Degradable Functional Poly(dimethylaminoethyl methacrylate) by Vinyl Oligomer Combination. *Angew. Chemie Int. Ed.* **53**, 6095–6100 (2014).
150. He, T., Yang, C. T., Jackson, A., Chandrasekharan, P., Shi, J., Rannard, S. P., Liu, Q. Synthesis and in vivo magnetic resonance imaging evaluation of biocompatible branched copolymer nanocontrast agents. *Int. J. Nanomedicine* **10**, 5895–5907 (2015).
151. Hatton, F. L., Tatham, L. M., Tidbury, L. R., Chambon, P., He, T., Owen, A., Rannard, S. P. Hyperbranched polydendrons: a new nanomaterials platform with tuneable permeation through model gut epithelium. *Chem. Sci.* **6**, 326–334 (2015).
152. Xu, Q., A. S., Venet, M., Gao, Y., Zhou, D., Wang, W., Zeng, M., Rotella, C., Li, X., Wang, X., Lyu, J., Rodriguez, B. J., Wang, W. Bacteria-Resistant Single Chain Cyclized/Knotted Polymer Coatings. *Angew. Chemie Int. Ed.* **58**, 10616–10620 (2019).
153. Namivandi-Zangeneh, R., Kwan, R. J., Nguyen, T. K., Yeow, J., Byrne, F. L., Oehlers, S. H., Wong, E. H. H., Boyer, C. The effects of polymer topology and chain length on the antimicrobial activity and hemocompatibility of amphiphilic ternary copolymers. *Polym. Chem.* **9**, 1735–1744 (2018).
154. Rolfe, B. E., Blakey, I., Squires, O., Peng, H., Boase, N. R. B., Alexander, C., Parsons, P. G., Boyle, G. M., Whittaker, A. K., Thurecht, K. J. Multimodal polymer nanoparticles with combined <sup>19</sup>F magnetic resonance and optical detection for tunable, targeted, multimodal imaging in vivo. *J. Am. Chem. Soc.* **136**, 2413–2419 (2014).
155. Tai, H., Wang, W., Vermonden, T., Heath, F., Hennink, W. E., Alexander, C., Shakesheff, K. M., Howdle, S. M. Thermoresponsive and photocrosslinkable PEGMEMA-PPGMA-EGDMA copolymers from a one-step ATRP synthesis. *Biomacromolecules* **10**, 822–828 (2009).
156. Dong, Y., Sigen, A., Rodrigues, M., Li, X., Kwon, S. H., Kosaric, N., Khong, S., Gao, Y., Wang, W., Gurtner, G. C. Injectable and Tunable Gelatin Hydrogels Enhance Stem Cell Retention and Improve Cutaneous Wound Healing. *Adv. Funct. Mater.* **27**, (2017).
157. A, S., Xu, Q., Zhou, D., Gao, Y., Vasquez, J. M., Greiser, U., Wang, W., Liu, W., Wang, W. Hyperbranched PEG-based multi-NHS polymer and bioconjugation with BSA. *Polym. Chem.* **8**, 1283–1287 (2017).

158. Chen, X., Li, R., Wong, S. H. D., Wei, K., Cui, M., Chen, H., Jiang, Y., Yang, B., Zhao, P., Xu, J., Chen, H., Yin, C., Lin, S., Lee, W. Y.-W., Jing, Y., Li, Z., Yang, Z., Xia, J., Chen, G., *et al.* Conformational manipulation of scale-up prepared single-chain polymeric nanogels for multiscale regulation of cells. *Nat. Commun.* **10**, 2705 (2019).
159. Zhao, T., Sellers, D. L., Cheng, Y., Horner, P. J., Pun, S. H. Tunable, Injectable Hydrogels Based on Peptide-Cross-Linked, Cyclized Polymer Nanoparticles for Neural Progenitor Cell Delivery. *Biomacromolecules* **18**, 2723–2731 (2017).
160. Yoshimatsu, K., Lesel, B. K., Yonamine, Y., Beierle, J. M., Hoshino, Y., Shea, K. J. Temperature-responsive ‘catch and release’ of proteins by using multifunctional polymer-based nanoparticles. *Angew. Chemie - Int. Ed.* **51**, 2405–2408 (2012).
161. Lee, S. H., Hoshino, Y., Randall, A., Zeng, Z., Baldi, P., Doong, R. A., Shea, K. J. Engineered synthetic polymer nanoparticles as IgG affinity ligands. *J. Am. Chem. Soc.* **134**, 15765–15772 (2012).
162. Hoshino, Y., Koide, H., Urakami, T., Kanazawa, H., Kodama, T., Oku, N., Shea, K. J. Recognition, neutralization, and clearance of target peptides in the bloodstream of living mice by molecularly imprinted polymer nanoparticles: A plastic antibody. *J. Am. Chem. Soc.* (2010). doi:10.1021/ja102148f
163. Pan, G., Guo, Q., Ma, Y., Yang, H., Li, B. Thermo-responsive hydrogel layers imprinted with RGDS peptide: A system for harvesting cell sheets. *Angew. Chemie - Int. Ed.* **52**, 6907–6911 (2013).
164. Ma, Y., Pan, G., Zhang, Y., Guo, X., Zhang, H. Narrowly dispersed hydrophilic molecularly imprinted polymer nanoparticles for efficient molecular recognition in real aqueous samples including river water, milk, and bovine serum. *Angew. Chemie - Int. Ed.* **52**, 1511–1514 (2013).
165. Kloxin, A. M., Kasko, A. M., Salinas, C. N., Anseth, K. S. Photodegradable Hydrogels for Dynamic Tuning of Physical and Chemical Properties. *Science* **324**, 59–63 (2009).
166. Hook, A. L., Chang, C. Y., Yang, J., Luckett, J., Cockayne, A., Atkinson, S., Mei, Y., Bayston, R., Irvine, D. J., Langer, R., Anderson, D. G., Williams, P., Davies, M. C., Alexander, M. R. Combinatorial discovery of polymers resistant to bacterial attachment. *Nat. Biotechnol.* **30**, 868–875 (2012).
167. Vining, K. H., Scherba, J. C., Bever, A. M., Alexander, M. R., Celiz, A. D., Mooney, D. J. Synthetic Light-Curable Polymeric Materials Provide a Supportive Niche for Dental Pulp Stem Cells. *Adv. Mater.* **1704486**, 1704486 (2017).
168. Mei, Y., Saha, K., Bogatyrev, S. R., Yang, J., Hook, A. L., Kalcioğlu, Z. I., Cho, S. W., Mitalipova, M., Pyzocha, N., Rojas, F., Van Vliet, K. J., Davies, M. C., Alexander, M. R., Langer, R., Jaenisch, R., Anderson, D. G. Combinatorial development of biomaterials for clonal growth of human pluripotent stem cells. *Nat Mater* **9**, 768–778 (2010).
169. Yan, M., Liang, M., Wen, J., Liu, Y., Lu, Y., Chen, I. S. Y. Single siRNA nanocapsules for enhanced RNAi delivery. *J. Am. Chem. Soc.* **134**, 13542–13545 (2012).
170. Yan, M., Du, J., Gu, Z., Liang, M., Hu, Y., Zhang, W., Priceman, S., Wu, L., Zhou, Z. H., Liu, Z., Segura, T., Tang, Y., Lu, Y. A novel intracellular protein delivery platform based on single-protein nanocapsules. *Nat. Nanotechnol.* **5**, 48–53 (2010).

171. Koide, H., Yoshimatsu, K., Hoshino, Y., Lee, S.-H., Okajima, A., Ariizumi, S., Narita, Y., Yonamine, Y., Weisman, A. C., Nishimura, Y., Oku, N., Miura, Y., Shea, K. J. A polymer nanoparticle with engineered affinity for a vascular endothelial growth factor (VEGF165). *Nat. Chem.* **9**, 715–722 (2017).
172. Tillberg, P. W., Chen, F., Piatkevich, K. D., Zhao, Y., Yu, C. C., English, B. P., Gao, L., Martorell, A., Suk, H. J., Yoshida, F., Degennaro, E. M., Roossien, D. H., Gong, G., Seneviratne, U., Tannenbaum, S. R., Desimone, R., Cai, D., Boyden, E. S. Protein-retention expansion microscopy of cells and tissues labeled using standard fluorescent proteins and antibodies. *Nat. Biotechnol.* **34**, 987–992 (2016).
173. Chen, F., Wassie, A. T., Cote, A. J., Sinha, A., Alon, S., Asano, S., Daugharthy, E. R., Chang, J. B., Marblestone, A., Church, G. M., Raj, A., Boyden, E. S. Nanoscale imaging of RNA with expansion microscopy. *Nat. Methods* **13**, 679–684 (2016).
174. Zhao, Y., Bucur, O., Irshad, H., Chen, F., Weins, A., Stancu, A. L., Oh, E. Y., Distasio, M., Torous, V., Glass, B., Stillman, I. E., Schnitt, S. J., Beck, A. H., Boyden, E. S. Nanoscale imaging of clinical specimens using pathology-optimized expansion microscopy. *Nat. Biotechnol.* **35**, 757–764 (2017).
175. Soeriyadi, A. H., Li, G.-Z., Slavin, S., Jones, M. W., Amos, C. M., Becer, C. R., Whittaker, M. R., Haddleton, D. M., Boyer, C., Davis, T. P. Synthesis and modification of thermoresponsive poly(oligo(ethylene glycol) methacrylate) via catalytic chain transfer polymerization and thiol–ene Michael addition. *Polym. Chem.* **2**, 815 (2011).
176. Baudry, R., Sherrington, D. C. Facile Synthesis of Branched Poly(vinyl alcohol)s. *Macromolecules* **39**, 5230–5237 (2006).
177. Bao, Y., Shen, G., Liu, X., Li, Y. RAFT polymerization of a novel allene-derived asymmetrical divinyl monomer: A facile strategy to alkene-functionalized hyperbranched vinyl polymers with high degrees of branching. *J. Polym. Sci. Part A Polym. Chem.* **51**, 2959–2969 (2013).
178. Jia, Y.-B. B., Ren, W.-M. M., Liu, S.-J. J., Xu, T., Wang, Y.-B. B., Lu, X.-B. B. Controlled Divinyl Monomer Polymerization Mediated by Lewis Pairs: A Powerful Synthetic Strategy for Functional Polymers. *ACS Macro Lett.* **3**, 896–899 (2014).
179. Butler, G. B., Myers, G. R. The Fundamental Basis for Cyclopolymerization. IV. Radiation Initiated Solid-State Polymerization of Certain Dimethacrylamides. *J. Macromol. Sci. Part A - Chem.* **5**, 135–166 (1971).
180. Costa, A. I., Barata, P. D., Prata, J. V. Radical cyclopolymerization of a divinylbenzyl-p-tert-butylcalix[4]arene derivative. *React. Funct. Polym.* **66**, 465–470 (2006).
181. Edizer, S., Veronesi, B., Karahan, O., Aviyente, V., Değirmenci, I., Galbiati, A., Pasini, D. Efficient Free-Radical Cyclopolymerization of Oriented Styrenic Difunctional Monomers. *Macromolecules* **42**, 1860–1866 (2009).
182. Ochiai, B., Ito, S., Endo, T. Chiral interaction between aromatic aldehydes and a polymer bearing large chiral rings obtained by cyclopolymerization of bisacrylamide. *Polym. J.* **42**, 138–141 (2010).
183. Sharma, A. K., Cornaggia, C., Pasini, D. Controlled RAFT Cyclopolymerization of Oriented Styrenic Difunctional Monomers. *Macromol. Chem. Phys.* **211**, 2254–2259 (2010).
184. Tang, W., Matyjaszewski, K. Kinetic Modeling of Normal ATRP, Normal ATRP with [CuII]0, Reverse

- ATRP and SR&NI ATRP. *Macromol. Theory Simulations* **17**, 359–375 (2008).
185. In *IUPAC Compendium of Chemical Terminology* (IUPAC). doi:10.1351/goldbook.CT07136
186. Saito, Y., Saito, R. The effect of the distance between neighboring vinyl groups on template polymerization. *Polymer* **52**, 3565–3569 (2011).
187. In *IUPAC Compendium of Chemical Terminology* (IUPAC). doi:10.1351/goldbook.M03706

### **Acknowledgements**

The authors acknowledge the Science Foundation Ireland (SFI) Principal Investigator Program (13/IA/1962) (to W.W.), National Science Foundation (NSF) Division of Materials Research (DMR) (1501324) (to K.M.), National Natural Science Foundation of China (NSFC) (51873179) (to W.W.), Senior Visiting Scholarship of State Key Laboratory, Fudan University (19FGJ07) (to W.W.), Irish Research Council (IRC) Employment-Based Postgraduate Programme (EBPPG/2018/159) (to J.L.), and University College Dublin (to Y.G.) for financial support. The authors apologize to those whose work is relevant but could not be cited owing to space limitations.

### **Author contributions**

Y.G. D.Z. and J.L. contributed equally to the research, writing and review of this article.

### **Competing interests**

The authors declare no competing interests.

### **Publisher's note**

Springer Nature remains neutral with regard to jurisdictional claims in published maps and institutional affiliations.

### **Peer review information**

*Nature Reviews Chemistry* thanks A. Zhukhovitskiy, H. Wei and the other, anonymous, reviewer(s) for their contribution to the peer review of this work.

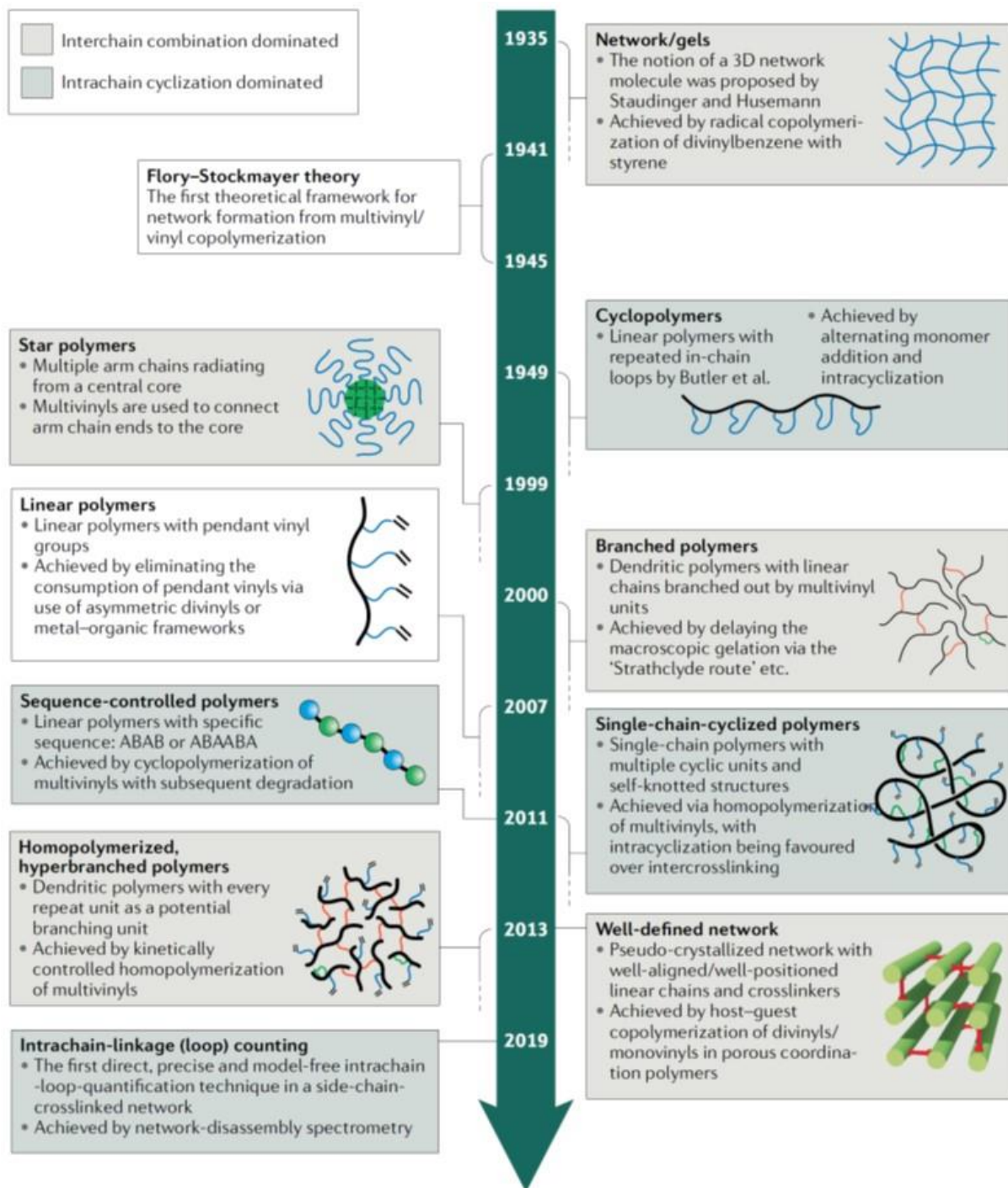
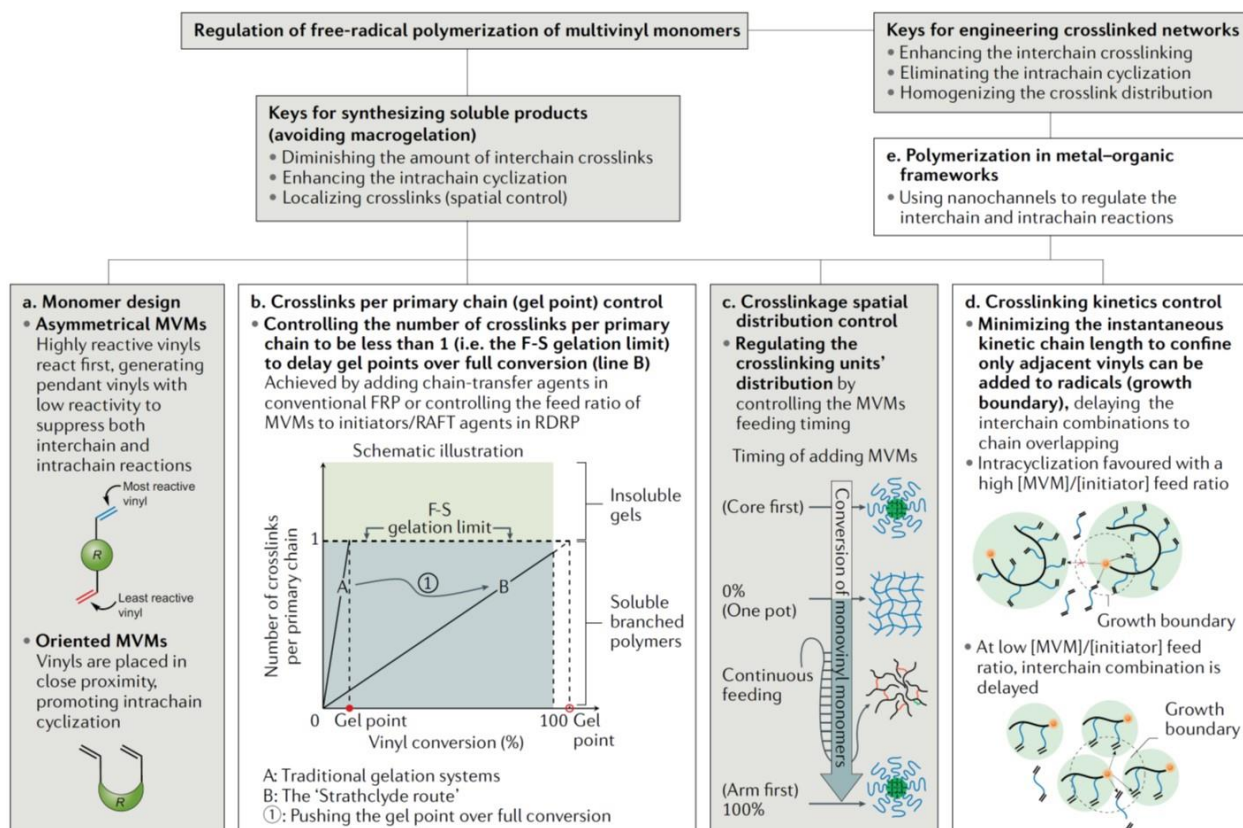


Figure 1. **Timeline of architecturally complex polymers by free radical polymerization of MVMs.** A brief summary of the major achievements in the field is given. The polymer architectures are described and further categorized as intra-chain cyclization dominated and inter-chain combination dominated classes. Part of this figure is adapted with permission from REF.<sup>16</sup>



**Figure 2. Strategies to control free radical polymerization of MVMs.** FRP is generally controlled by regulating the inter-chain crosslinking, intra-chain cyclization and spatial distribution of crosslinks. To synthesize soluble products, it is key to avoid macrogelation by diminishing the inter-chain combinations, enhancing intra-chain cyclization and localizing the crosslinks. Contemporary experimental strategies include a) monomer design, b) control of crosslinks per primary chain (gel point control), c) control of the spatial distribution of crosslinks, d) kinetic control of crosslinking reactions, and e) use of nanochannels. a) The inter-chain and intra-chain crosslinking can be readily regulated by designing asymmetric MVMs or orienting the vinyl moieties in a close proximity. b) The gel point can be delayed until full conversion by controlling the crosslinks per primary chain. c) The crosslinks spatial distribution can be regulated by tailoring the monomer feeding policies. d) The control of the instantaneous kinetic chain length provides an approach to regulate the chain growth boundary to delay the gel point. e) The use of metal-organic frameworks can achieve exclusively intermolecular reaction or intramolecular cyclization, yielding well-defined network or cyclopolymers.

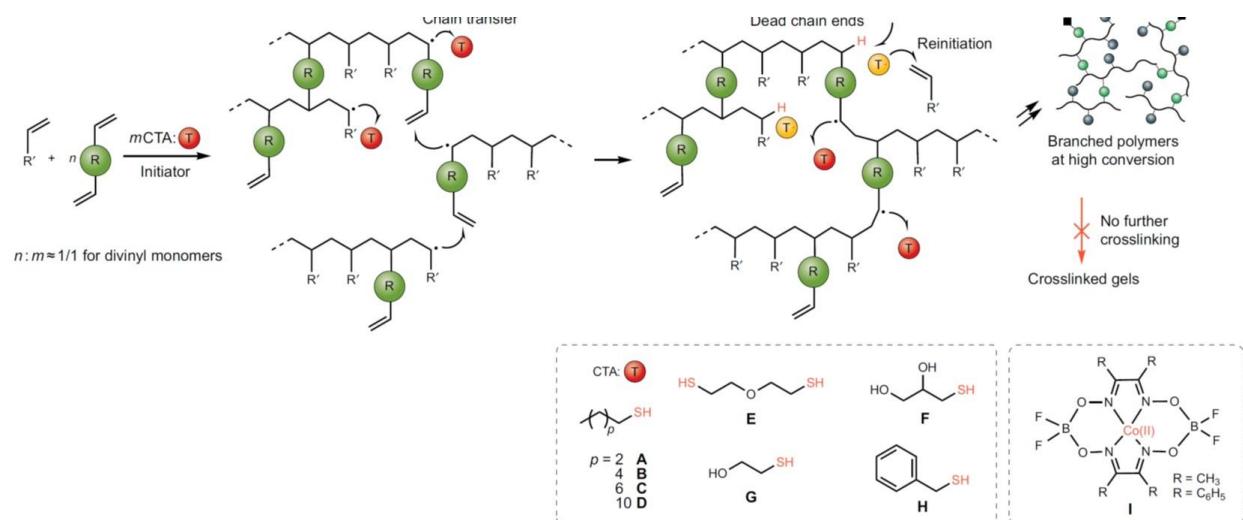


Figure 3. The “Strathclyde route” for synthesis of branched polymers. In conventional FRP, the added chain transfer agent (CTA) (A–I)<sup>38,39,175,176</sup> terminates the propagating chain through chain transfer reaction, keeping the primary chain length short and the average number of crosslinkers per primary chain less than 1 thus to avoid the macrogelation



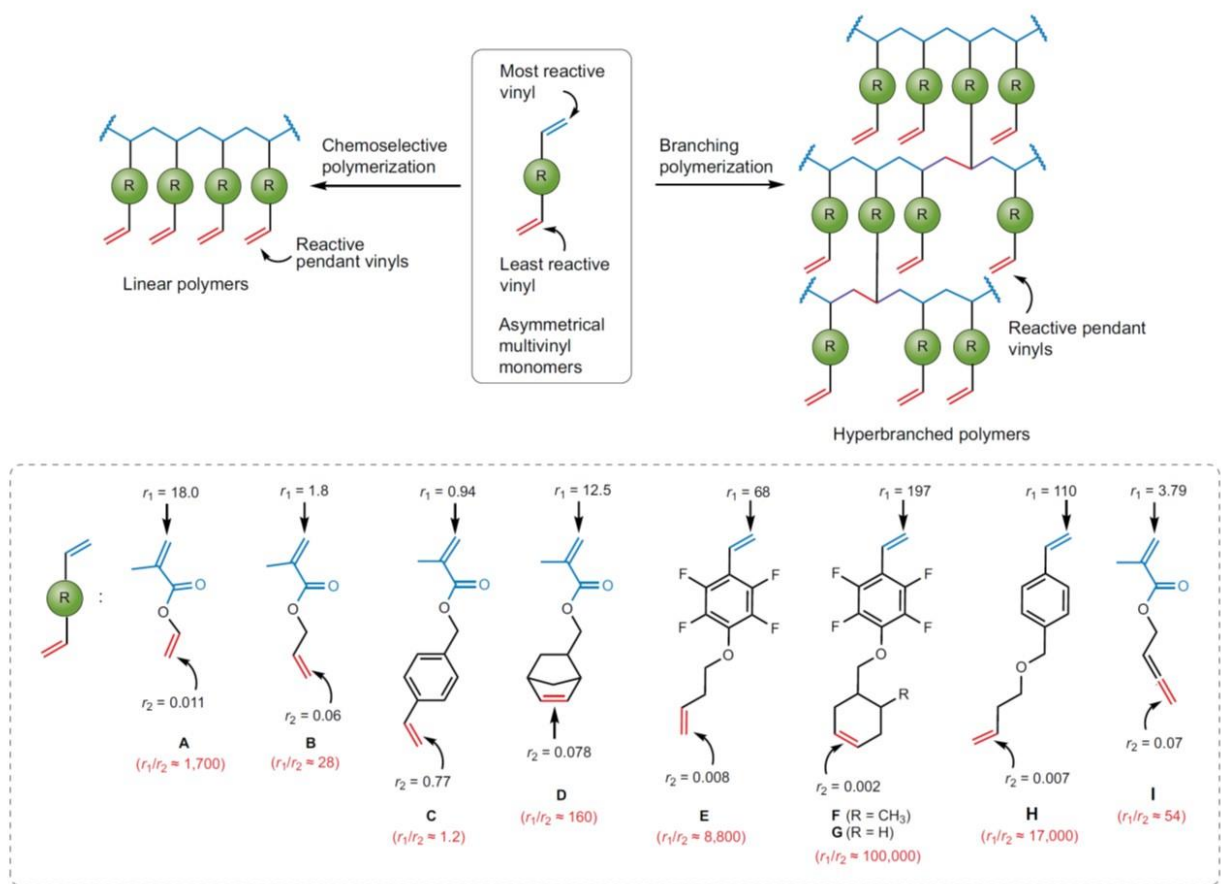


Figure 4. **Chemoselective polymerization and branched polymerization of asymmetrical monomers.** The reactivity difference of vinyls in an asymmetrical MVM (A~I<sup>65,66,69,177,178</sup>) can be used to regulate the reaction kinetics, as high reactive vinyls are reacted first (*via* monomer addition reaction) leaving the less reactive one reserved as pendent functional groups (producing linear polymer) or consumed in a delayed manner (generating branched polymers). Thus it is critical to have the reactivity ratio for each pair of vinyl moieties ( $r_1/r_2$ , calculated based on Alfrey-Price theory<sup>60</sup>) be significantly different.

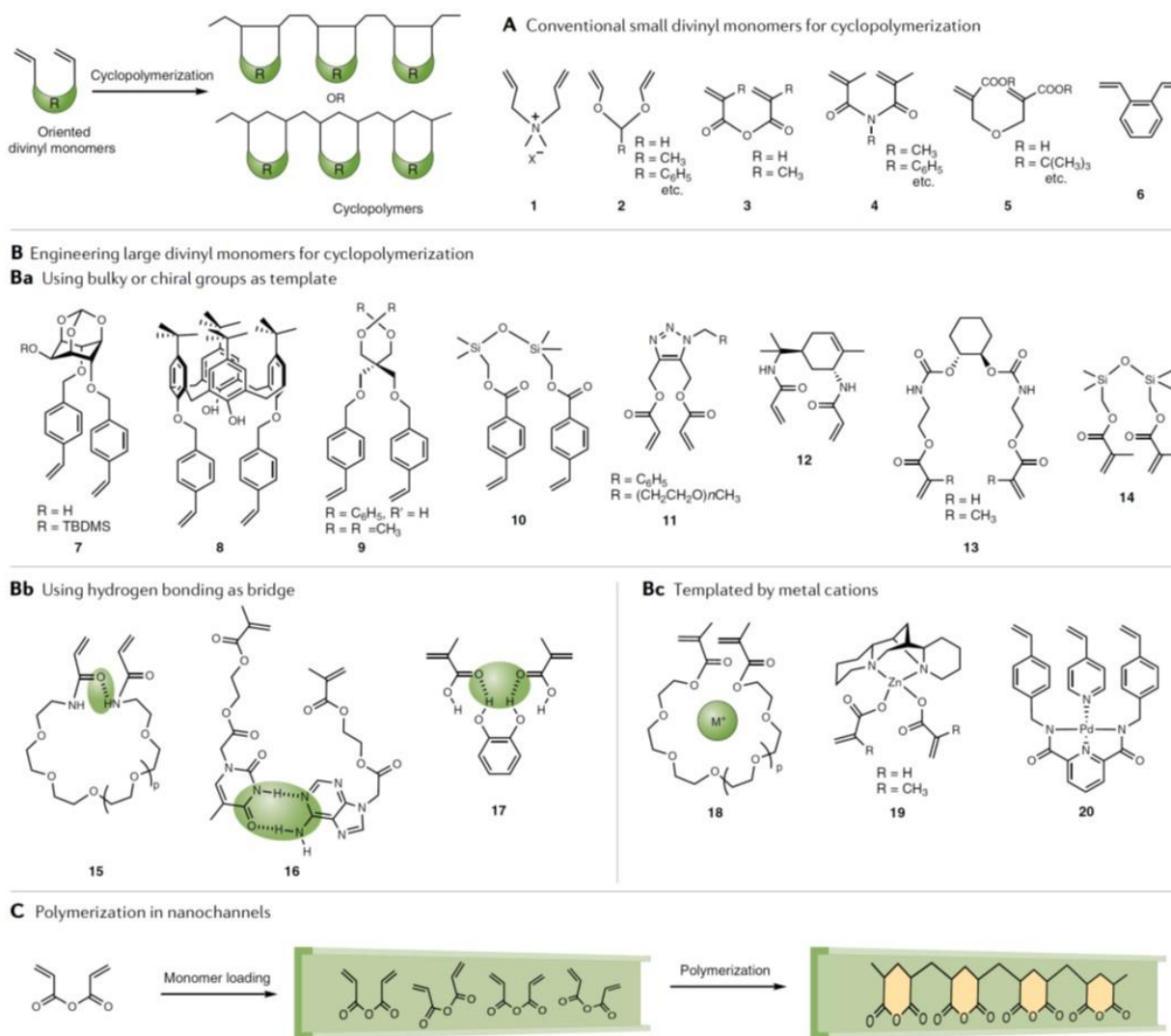
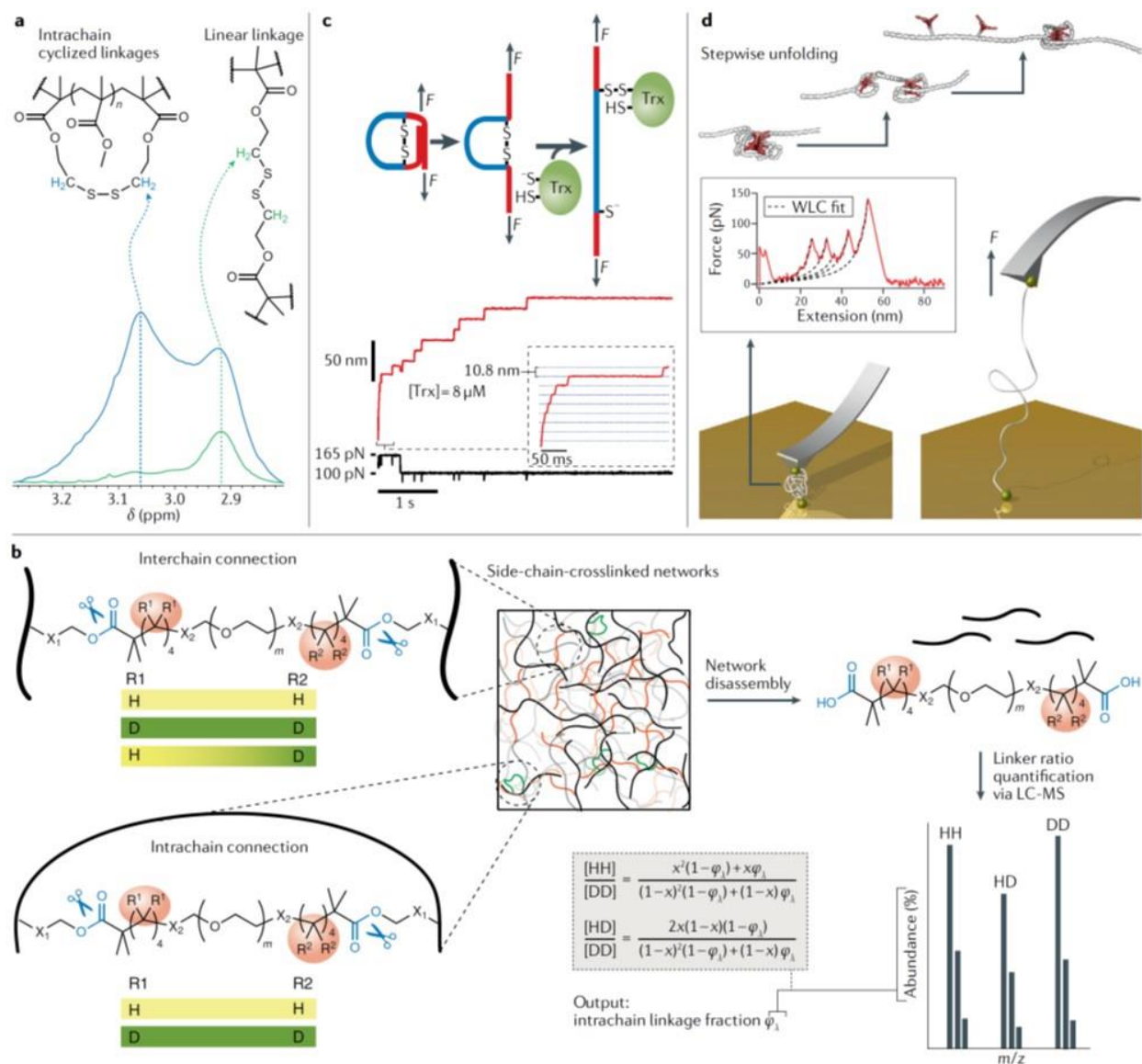


Figure 5. **Contemporary experimental strategies to engineer MVMs for cyclopolymerization.** Cyclopolymerization can be achieved by either using small DVMs (A)<sup>87,91–93,95,96,179</sup> or by orienting the vinyl moieties close to one another through the use of a bulky template (Ba),<sup>100–105,180–183</sup> a metal template (Bc),<sup>106–108</sup> by exploiting hydrogen bonding (Bb)<sup>110–112</sup> or by constraining the reacting monomers in nanochannels (C)<sup>115</sup>.



**Figure 6. Representative advanced techniques for identifying and quantifying intra- and inter-chain connections.** **a** Partial  $^1\text{H-NMR}$  spectra showing the different thiamethylene signals for the residues of fully reacted disulfide-based dimethacrylate forming an intramolecular cycle or an intermolecular branch. Adapted with permission from REF.<sup>121</sup> **b** Schematic of the network disassembly spectrometry strategy for the calculation of inter- and intra-chain connections in sidechain-crosslinked polymer networks based on counting the different isotope labelled linkers after degradation.  $x/(1-x)$  is the molar ratio of the normal (H) and deuterium (D)-labelled primary chains. Intra-chain connections can only generate unlabeled (HH) and fully labelled (DD) linkages. Interchain connections result in all three possibilities (HH, DD and HD). The mass difference of these fragments can be used to calculate the percentage of intra-chain connections. Adapted with permission from REF.<sup>125</sup> **c** Single-molecule force spectroscopy for protein unfolding with the cleavage of intra-chain disulfide bridges, and the typical extension-time curve recording the disulfide bond breakage by a 10.8 nm chain elongation, correlated to the residue length looped by disulfide bonds. Adapted with permission from REF.<sup>133</sup> **d** Schematic illustrations of the mechanical unfolding experiment on single chain polymeric nanoparticles and the typical force-extension curve showing the unfolding of the intra-chain bridges. Adapted with permission from REF.<sup>131</sup>

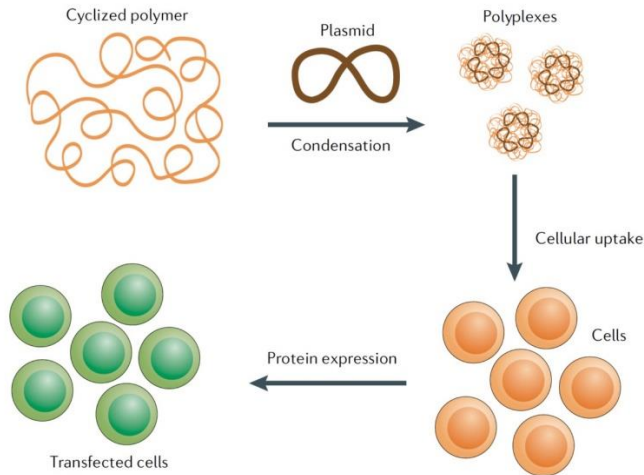


Figure 7. **Gene transfection with a cyclized polymer as the delivery vector.** The cyclized polymer condenses the plasmid to form nano-sized and positively charged polyplexes. These are taken up by cells through endocytosis and thus mediate functional protein expression inside cells.

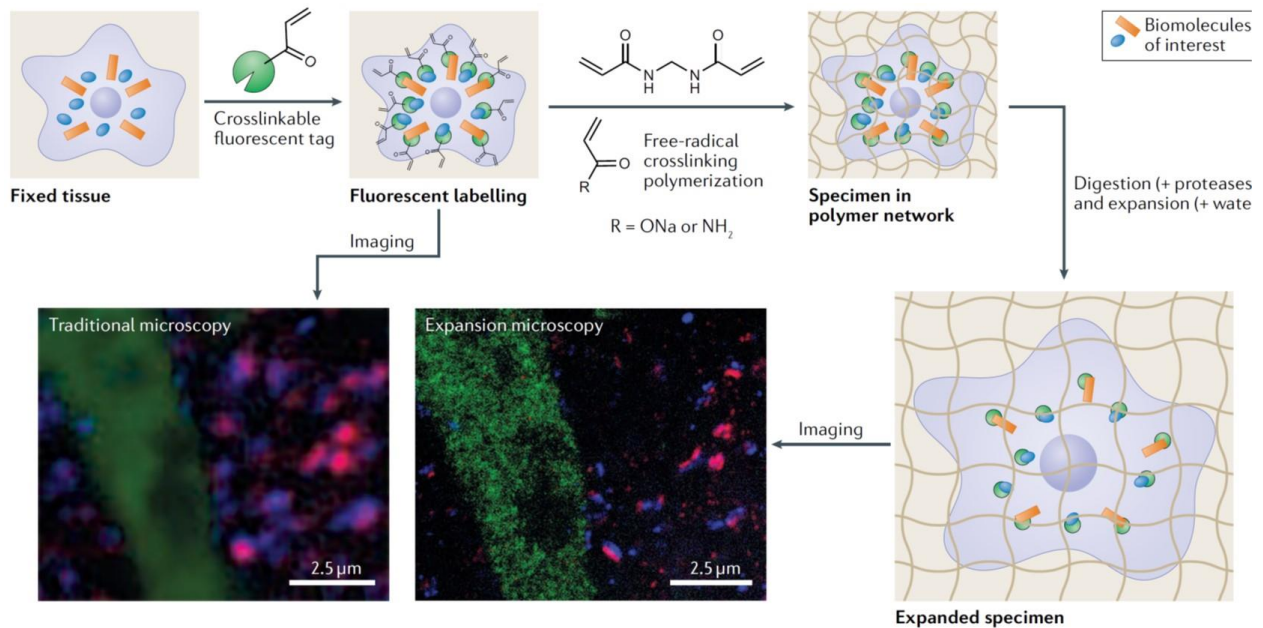


Figure 8. **Expansion Microscopy.** Biomolecules of interest in prefixed cells or tissues are first functionalized using a fluorescent tag carrying a vinyl moiety. Specimens are then infused with initiators, comonomers and divinyl crosslinkers: *N,N'*-methylenebisacrylamide, which are further crosslinked through free radical polymerization. After proteolysis, the tissue-polymer composite are swelled in water, resulted in 4.5-fold linear expansion, enabling high resolution imaging. Reproduced with permission from REF.<sup>15</sup>.

### [b1] Flory-Stockmayer (F-S) theory

In the 1940s Flory<sup>13</sup> and Stockmayer<sup>14</sup> outlined the first theoretical framework for the definition and calculation of gel point based on the mean-field statistical theory. For the radical (co)polymerization of DVMs, they put forward a mathematical expression of the gel point, based on an ideal polymer gel system with two assumptions: i) all vinyl groups have equal and independent reactivity, and ii) intramolecular cyclization reactions are neglected. This resulted in the following equation:

$$v_c = \alpha_c \rho (\lambda_w - 1) = 1 \quad (1)$$

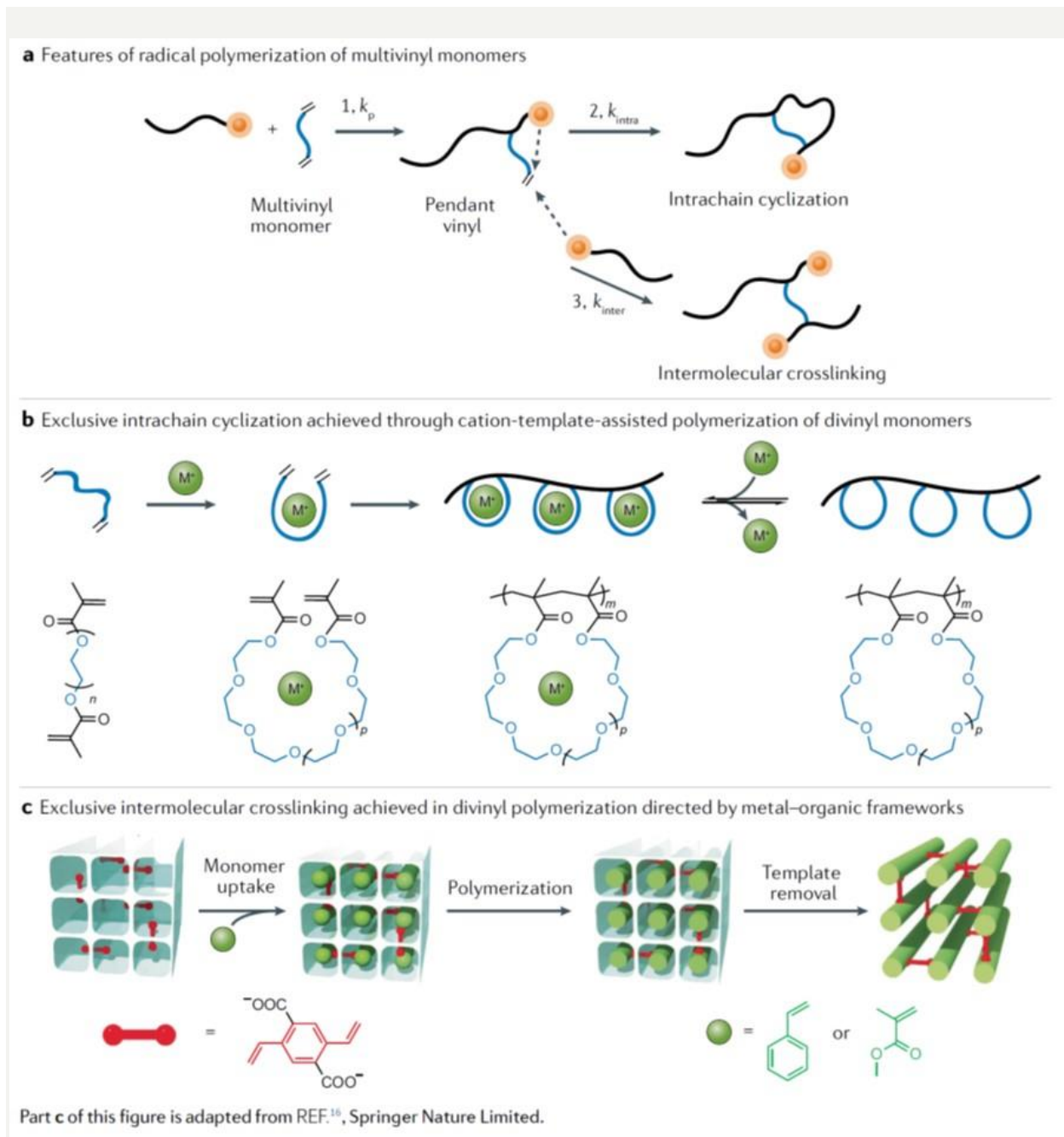
where  $v$  is the weight-average number of crosslinks for each primary chain (equal to 1 at the critical gelation state),  $\alpha$  is the extent of reaction of vinyl groups. The subscript  $c$  is added to represent the critical gelation state,  $\rho$  is the initial mole fraction of vinyls in divinylmonomers (within a mixture of divinylmonomers and vinyl monomers), and  $\lambda_w$  is the weight-average polymerization degree of primary chains.

These assumptions greatly simplify the mathematical analysis of the model but also limit its practical application to a large extent. Discrepancies are frequently found between the Flory–Stockmayer calculations and experimentally observed gel points and are attributed either to intramolecular cyclization, or varied vinyl reactivity, or both.

### [b2] Radical polymerization of multivinyl monomers

The radical polymerization of MVMs is a special field of free radical polymerization (FRP) with unique mechanistic processes and special reaction kinetics, such as cross-linking, cyclization, autoacceleration, reaction diffusion-controlled termination. All of these features originate from the generation of polymerizable pendent vinyl moieties on the growing chain (reaction **1** in the figure a), and these pendent vinyls can continue to react with propagating radicals through either intra-chain cyclization or inter-chain crosslinking. Intra-chain cyclization occurs when a pendent vinyl reacts with a radical in the same chain- leaving behind a loop in the propagating chain (ring-closing reaction, reaction **2** of the figure a). Intra-chain cyclization is a special type of chain growth which elongates the length of kinetic chains without increasing their molecular weight. Intermolecular crosslinking is a type of bimolecular reactions where pendent vinyl groups react with radicals from other propagating chains resulting in the combination of different primary chains and ultimately causing the change of the system from soluble sols to insoluble gels (reaction **3** of the figure a). The seemingly trivial ability of one repeat unit to undergo multiple times of chain propagations enables the formation of a range of novel macromolecular materials, ranging from a common network to the more complex architectures.

It is critical to evaluate (and ultimately attempt to control) the rates of these two coexisting and competing reactions in order to synthesize architecturally well-defined polymers. The experimental regulation of these two reactions has been under extensive investigation, with the ultimate goal of efficient synthesis of either intra-chain cyclization dominated, or inter-molecular crosslinking dominated polymer topology. Figure b and c illustrate two elegant strategies towards that end. To achieve exclusively intramolecular cyclization with non-specialized MVMs, Sawamoto and coworkers used a cation template to direct the monomers into a pseudocyclic conformation. This brings the two intramolecular vinyl groups into proximity so that they are suitably positioned for intramolecular cyclization instead of intermolecular crosslinking, yielding linear cyclopolymers with large in-chain PEG rings.<sup>110</sup> Kitagawa and coworkers further achieved conditions for inter-molecular only crosslinking reactions by embedding the divinyl monomers (DVMs) into the structure of metal-organic frameworks. Subsequent radical polymerization of vinyl monomers inside the nanochannels consumed DVMs solely by inter-chain crosslinking because the two vinyl moieties are physically separated with no intra-chain cyclization reactions being possible.<sup>16</sup> Part of this figure is adapted with permission from REF.<sup>16</sup>



**[b3] Box 3. The growth boundary model for controlled homopolymerization of multivinyl monomers**

To enable the kinetic and spatial manipulation of chain growth related reactions, including monomer addition, intrachain cyclization and intermolecular crosslinking (Box 2– Figure a), it is important to consider the instantaneous kinetic chain length of ATRP, which is defined as the number of double bonds added during one activation cycle<sup>184</sup>

$$\nu = \frac{R_p}{R_{\text{deact}}} = \frac{k_p[M]}{k_{\text{deact}}[\text{Cu}^{\text{II}}/\text{ligand}]} \quad (2)$$

The instantaneous kinetic chain length ( $\nu$ ) of ATRP generally represents the length that a growing chain can reach in a single activation/deactivation cycle, and may be intuitively termed the growth boundary.<sup>59,116,119</sup>

To produce architecturally complex polymers, it is critical to keep this kinetic chain length short and thus avoid the early stage gelation, as demonstrated in deactivation enhanced (DE)-ATRP of MVMs (Figure below). Under conventional FRP or normal ATRP conditions, the kinetic chain length, and thus the growth boundary is large and

allows a large number of vinyl groups to be added to an active center in each active cycle (Figure 2d). All of the vinyl groups within the growth boundary have the chance to be react, including pendent vinyl groups in other polymer chains. This results in the rapid generation of high molecular weight polymer chains. The overlap with the growth boundary of other active polymers results in significant inter-chain combination, quickly yielding an insoluble gel, in accordance with Flory–Stockmayer theory. However, the DE approach retains a larger amount of deactivator species ( $\text{Cu}^{\text{II}}$ /ligand as shown here), and thus the instantaneous kinetic chain length is kept small. This small growth boundary confines the addition of the active center to only the very few closest vinyl groups before deactivation occurs, and hence keeps the polymer chains growing in a limited space (Figure 2d). In this way, unlike a typical FRP, the deactivation strategy avoids the rapid formation of large polymer chains combinations of multiple chains in the early stages of the polymerization reaction.

With a small growth boundary, the manipulation of the chain dimension and chain volume concentration can potentially regulate the occurrence of intermolecular crosslinking and intra-chain cyclization. The chain dimension and chain volume concentration are closely correlated with the initial molar feed ratio of DVMs to initiator ( $N_k$ ). In systems with small  $N_k$  values (e.g. 2),<sup>59</sup> a large amount of initiator is added and as a result of the small growth boundary, the addition of a large number of monomers to a single primary chain is avoided. Instead, the monomers are predominately converted to short oligomers in a controlled fashion. Subsequent intermolecular combination produces hyperbranched polymers with a high branching ratio and vinyl functional groups.

In systems with large  $N_k$  values (e.g. 100),<sup>116</sup> a small number of short primary chains are generated in the the early stages of reaction. Thus, for a specific active center in its active cycle, the nearest vinyl groups are most likely to be monomeric vinyl groups or pendent vinyl groups in the same chain, respectively. Reaction with these proximal vinyl groups corresponds to the chain propagation and intra-chain cyclization. In this situation the intramolecular cyclization is kinetically favored over the intermolecular crosslinking. The benefits of a high proportion of intramolecular consumption of pendent vinyl groups are twofold: i) monomer conversion before gelation can be significantly increased; and ii) single-chain cyclized polymers can be generated if the polymerization is terminated in a timely fashion, before intermolecular crosslinking occurs.

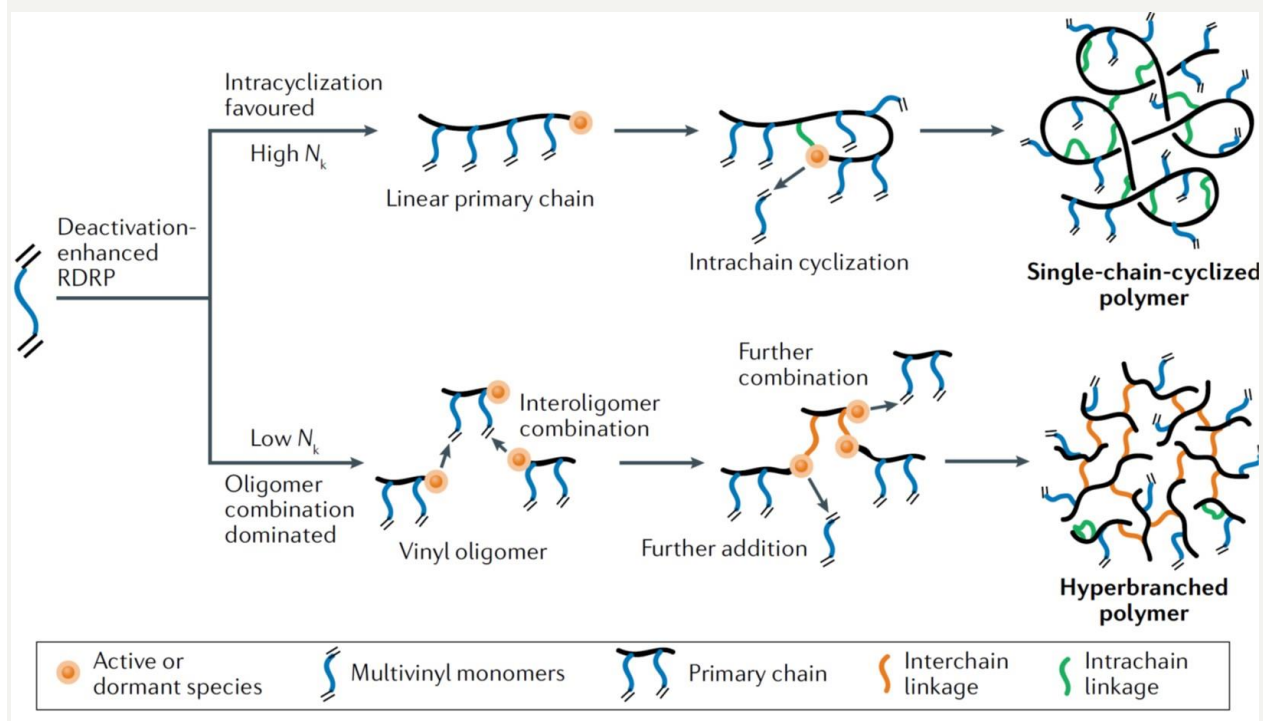


## Table of contents

During free radical polymerization, the regulation of intermolecular crosslinking and intramolecular cyclization enables the construction of complex polymer architectures. This Review summarizes methods to achieve this control and techniques to analyse the sub chain connections. Finally, it discusses exemplary biomedical applications of the complex polymer products.

## List of glossary term

**Intramolecular cyclization:** According to IUPAC,<sup>185</sup> crosslink is defined as a small region that connects two or more different polymer chains. Intramolecular reaction here is also ascribed as a special crosslinking reaction, because it produces a similar linking unit that bridges two different monomers at the same primary chain together, forming a loop structure.

**Degree of branching (DB):** In radical polymerization of MVMs, degree of branching is defined as the number of branch points (i.e. fully reacted MVMs) per repeat unit, as quantified by nuclear magnetic resonance<sup>59</sup> or through degradation<sup>46</sup>.

**“5 Å rule”:** “5 Å rule” that it is necessary to keep the distance between the two vinyl within 5 Å to ensure the enhancement of intramolecular cyclization.<sup>186</sup>

**Instantaneous kinetic chain length:** The number of double bonds added during one activation-deactivation cycle in ATRP<sup>184</sup> (Equation 2 of Box 3)

**“Grafting-from” polymerization.** A type of polymerization process in which initiating moieties are covalently bonded to the main polymer backbone and monomers are polymerized as side chains.

**Mark–Houwink exponent ( $\alpha$ ):** A constant from Mark–Houwink equation, which correlates the intrinsic viscosity ( $[\eta]$ ) of polymer with its molecular weight ( $M$ ):  $[\eta]=kM^\alpha$ .<sup>187</sup>  $\alpha$  values depend on the configuration of polymer chains in the solvent environment.